

YIELDING AND FLOW IN VANADIUM

BY

LEONARD ANGUS SIMPSON  
B. Sc., The University of British Columbia, 1961

A THESIS SUBMITTED IN PARTIAL FULFILMENT OF

THE REQUIREMENTS FOR THE DEGREE OF

MASTER OF SCIENCE

in the Department

of

METALLURGY

We accept this thesis as conforming to the  
standard required from candidates for the  
degree of MASTER OF SCIENCE.

Members of the Department  
of Metallurgy

THE UNIVERSITY OF BRITISH COLUMBIA

April, 1963

In presenting this thesis in partial fulfilment of the requirements for an advanced degree at the University of British Columbia, I agree that the Library shall make it freely available for reference and study. I further agree that permission for extensive copying of this thesis for scholarly purposes may be granted by the Head of my Department or by his representatives. It is understood that copying or publication of this thesis for financial gain shall not be allowed without my written permission.

Department of Metallurgy

The University of British Columbia,  
Vancouver 8, Canada.

Date April 11th, 1963

## ABSTRACT

An investigation of the characteristics of yielding and flow in polycrystalline and single crystal vanadium has been carried out. The effect of grain size, temperature and strain rate on these properties was studied.

It was found that there is no similarity between the mechanisms of yielding and flow in vanadium which is in disagreement with work on iron.

The results of tensile tests suggest that the mechanism controlling thermally activated flow is probably either the Peierls-Nabarro force or the non-conservative motion of vacancy jogs. Some inadequacies of these mechanisms suggest that there may not be a single mechanism controlling thermally activated flow.

Yield points were observed in the stress-strain curve upon re-loading a tensile specimen under certain conditions and these are explained in terms of Snoek ordering.

## ACKNOWLEDGEMENT

The author wishes to thank Dr. J. A. Lund and Dr. E. Teghtsoonian for their guidance and assistance in the interpretation of this research. Thanks are also due to Mr. R. J. Richter for technical assistance and to fellow graduate students for many helpful discussions.

Financial aid for this project was received in the form of The Aluminium Laboratories Limited Fellowship and National Research Council Grant No. A-1463. This assistance is gratefully acknowledged.

## TABLE OF CONTENTS

	Page
I. INTRODUCTION AND PREVIOUS WORK . . . . .	1
A. Introduction . . . . .	1
B. Previous Work . . . . .	2
II. EXPERIMENTAL . . . . .	11
A. Material . . . . .	11
B. Zone Refining . . . . .	12
C. Specimen Preparation . . . . .	13
1. Machining . . . . .	13
2. Electropolishing . . . . .	13
3. Grain Size Determination and Control . . . . .	13
D. Tensile Testing . . . . .	14
E. Temperature Control . . . . .	17
III. EXPERIMENTAL RESULTS . . . . .	19
A. Polycrystalline Material . . . . .	19
1. Grain Growth . . . . .	19
2. Hall-Petch Equation . . . . .	20
3. Strain Rate Change Tests . . . . .	26
4. Temperature Change Tests . . . . .	27
5. "Pseudo" Yield Points . . . . .	31
6. Rate Equation . . . . .	34
B. Single Crystals . . . . .	42
1. Zone Refining . . . . .	42

## TABLE OF CONTENTS Continued

	Page
2. Slip Systems . . . . .	44
3. Strain Rate Change Tests . . . . .	46
4. Temperature Change Tests . . . . .	51
5. Rate Equation . . . . .	51
6. Yield Points . . . . .	54
C. Summary of Results . . . . .	56
IV. DISCUSSION . . . . .	58
A. Hall-Petch Equation . . . . .	58
B. Thermally Activated Flow . . . . .	59
1. Intersection With a Forest . . . . .	60
2. Impurity Atoms . . . . .	62
3. Cross Slipping of Screw Dislocations . . . . .	64
4. Peierls-Nabarro Force . . . . .	64
5. Non-Conservative Motion of Jogs in Screw Dislocations . . . . .	67
6. Comparison Between Polycrystals and Single Crystals . . . . .	69
7. Mechanism . . . . .	70
C. Yield Points . . . . .	73
V. CONCLUSIONS . . . . .	77
VI. RECOMMENDATIONS FOR FURTHER WORK . . . . .	78
VII. APPENDICES . . . . .	79
VIII. BIBLIOGRAPHY . . . . .	87

## LIST OF FIGURES

No.		Page
1.	Effect of the concentration of C + N in solution on $\sigma_0$ in Fe, after Heslop and Petch . . . . .	3
2.	Illustration of grain-to-grain yielding . . . . .	5
3.	Force-distance curve for thermally activated flow . . . . .	7
4.	Method of grain size measurement, specimen 9B, 210X . . . . .	15
5.	Drawing of grips used in tensile testing . . . . .	16
6.	Assembly for testing at 100°C . . . . .	17
7.	Inhomogeneous grain sizes after drawing, rod #2, 110X . . . . .	20
8.	Typical load-elongation curve for vanadium polycrystal . . . . .	21
9.	Dependence of yield stress and flow stress on grain size at 25°C . . . . .	22
10.	Dependence of lower yield stress on grain size . . . . .	24
11.	Typical load-elongation curve for a strain rate change test . . . . .	25
12.	Method of extrapolation to obtain change in flow stress . . . . .	26
13.	$\Delta \tau_a$ for an increase in $\dot{\epsilon}$ vs. $\tau_a$ for polycrystals . . . . .	28
14.	$\Delta \tau_a$ for an increase in $\dot{\epsilon}$ vs. $\tau_a$ and $\epsilon$ for polycrystals . . . . .	29
15.	$\Delta \tau_a$ for an increase in strain rate vs $\epsilon$ for polycrystals . . . . .	30
16.	$\Delta \tau_a$ for a decrease in temperature vs $\epsilon$ and $\tau_a$ for polycrystals. . . . .	32
17.	Load-elongation curves showing yield points . . . . .	33
18.	Method of extrapolation through yield points . . . . .	34
19.	Activation volume vs. flow stress . . . . .	36
20.	Activation volume vs. temperature . . . . .	37
21.	Energy, H, vs. $\epsilon$ . . . . .	38
22.	Thermally activated component of $H^0$ , $\Delta Q$ , vs. $\epsilon$ . . . . .	39

## LIST OF FIGURES Continued

No.		Page
23.	Pre-exponential factor A vs. $\epsilon$ for polycrystals . . . . .	40
24a.	Strain rate sensitivity of $\tau_a$ vs. temperature . . . . .	41
24b.	$\Delta Q$ vs. temperature for single crystals . . . . .	41
25a.	Laue photograph of sufficiently polished specimen . . . . .	43
25b.	Laue photograph of insufficiently polished specimen . . . . .	43
26.	Orientation of tensile axis of single crystals . . . . .	44
27.	Gas holes in single crystal specimens . . . . .	45
28.	Typical slip traces on single crystal specimen 6A, 210X . . . . .	45
29.	$\Delta \tau_a$ for an increase in $\dot{\epsilon}$ vs. $\tau_a$ for single crystals . . . . .	47
30.	$\Delta \tau_a$ for an increase in $\dot{\epsilon}$ vs. $\epsilon$ for single crystals . . . . .	48
31.	Twin markings on surface of single crystal . . . . .	50
32.	Laue photograph showing slits in spots due to twins . . . . .	50
33.	$\Delta \tau_a$ for a decrease in temperature vs $\tau_a$ for single crystals . . . . .	52
34.	$\Delta \tau_a$ for a decrease in temperature vs. $\tau_a$ for single crystals . . . . .	53
35.	Strain rate sensitivity of the flow stress vs. temperature sensitivity to find $\ln(A/\dot{\epsilon})$ . (equation (15)) . . . . .	55
36.	Transmission electron micrograph of dislocations in silicon iron, after Low and Turkalov . . . . .	65
37.	Formation of a dislocation kink in a Peierls force field . . . . .	66

## LIST OF TABLES

No.		Page
I.	Summary of Previous Work . . . . .	10
II.	Analysis of Material . . . . .	11
III.	Possible Slip Systems . . . . .	46
IV.	Summary of Results . . . . .	57

## I. INTRODUCTION AND PREVIOUS WORK

### A. Introduction

One of the most remarkable properties inherent in a body centered cubic metal is the marked temperature dependence of its strength. This has evoked considerable interest and many investigators have tried to analyze and explain this property.

Most of the investigations have been centered about the temperature dependence of the yield strength and have not been very productive in explaining the detailed mechanisms of deformation. Most of this work has been concerned with iron while the other body centered cubic metals have received relatively little attention.

The adoption of rate theory to explain thermally activated flow has led to an intensified attack on the problem of determining the deformation mechanisms in these metals. This method, first used to study f.c.c. metals, has been adapted to b.c.c. metals during the past four years. This has resulted in a number of publications on the flow mechanisms in iron, tantalum and columbium.

The problem of establishing a single mechanism as the one controlling thermally activated flow is rather difficult and current authors are in disagreement on many points. However, it must be borne in mind that this study is still in the embryo stage and a vast quantity of experiments is required before a sound theory can be devised.

It is, therefore, the object of this thesis to add to this pool of knowledge a description of the temperature dependent deformation

Properties of vanadium. It is intended to make a comparison of these properties between polycrystals and single crystals and also to investigate the role of grain size in the yielding and flow of vanadium.

B. Previous work

This investigation will be concerned with the two experimentally derived equations:

$$\sigma_{LY} = \sigma_i^o + \sigma^{o*} + k_{LY} d^{-1/2} \quad (1)$$

$$\sigma_{f1} = \sigma_i + \sigma^* + k_{f1} d^{-1/2} \quad (2)$$

where  $\sigma_{LY}$  is the lower yield stress, that is, the lowest point on the stress-strain curve after the beginning of plastic deformation.

$\sigma_{f1}$  is the flow stress, that is, the stress required to maintain plastic deformation at any given strain.

$\sigma_i$ ,  $\sigma_i^o$  are athermal friction stresses opposing dislocation motion.

$\sigma^*$ ,  $\sigma^{o*}$  are temperature dependent friction stresses opposing dislocation motion.

$k_{f1}$ ,  $k_{LY}$  are the slopes of plots of  $\sigma_{f1}$  and  $\sigma_{LY}$  against  $d^{-1/2}$ .  $d^{-1/2}$  is the mean grain diameter.

In earlier work  $\sigma_i^o$  and  $\sigma^{o*}$  have been studied as a single parameter,  $\sigma_o^o$ , and equation (1) has been used in the form

$$\sigma_{LY} = \sigma_o^o + k_{LY} d^{-1/2} \quad (3)$$

This is known as the Hall-Petch equation and was obtained experimentally by Petch<sup>1</sup> who followed up some earlier work by Hall<sup>2</sup>. Petch, who worked with polycrystalline iron supplemented his original work with

two more papers<sup>3,4</sup> in which he discussed the term  $\sigma_o^o$ . By varying the C + N content in solution he obtained the plots shown in Figure 1.

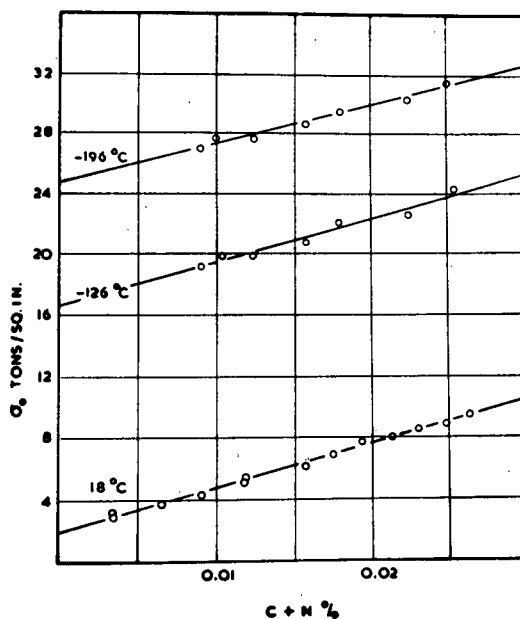


Figure 1. Effect of the concentration of C + N in solution on  $\sigma_o^o$  in Fe, after Heslop and Petch.

Because the slopes were the same at all temperatures, Petch concluded that the effect of interstitial atoms on the friction stress is independent of temperature. Therefore the interstitials would contribute to  $\sigma_i$  in equations (1) and (2).

Other factors contributing to  $\sigma_i$  are long range elastic stress fields which are created by the dislocation networks.  $\sigma_i$  therefore, will depend on temperature only through the elastic modulus.

A recent publication by Conrad and Schoeck<sup>5</sup> gives evidence that the mechanisms for yielding and flow might be the same. A series of tests was performed on polycrystalline iron from which the lower yield stress and the flow stress at 5% strain were plotted against  $d^{-1/2}$ . This resulted in similar values for  $k$  in the two plots. It was also observed that  $k$  was independent of temperature over a range from 100°K to 300°K. Data from Petch<sup>6</sup> also indicates a temperature independence of  $k_{LY}$  from 194°K to 300°K. Conrad and Schoeck interpreted the similarity between  $k_{LY}$  and  $k_{f1}$ , and the identical temperature dependences of  $\sigma_{f1}$ ,  $\sigma_{LY}$  and  $\sigma_i$ , as indicating that the same dislocation mechanism is involved in yielding as in flow.

The temperature independence of  $k_{LY}$  has evoked considerable interest. Cottrell<sup>7</sup> has explained the significance of  $k_{LY}$  in the following way. When a dislocation source is unpinned, it releases an avalanche of dislocations into the grain and these dislocations pile up at a grain boundary. Their stress concentration acts on sources in the next grain and the process is repeated. According to Cottrell, the sources are pinned by interstitial atoms.

The stress concentration due to a pile up on a source a distance  $l$  ahead of the pile up is given by

$$\left(\sigma_{LY} - \sigma_o\right) \left(\frac{d}{2l}\right)^{1/2} \quad (4)$$

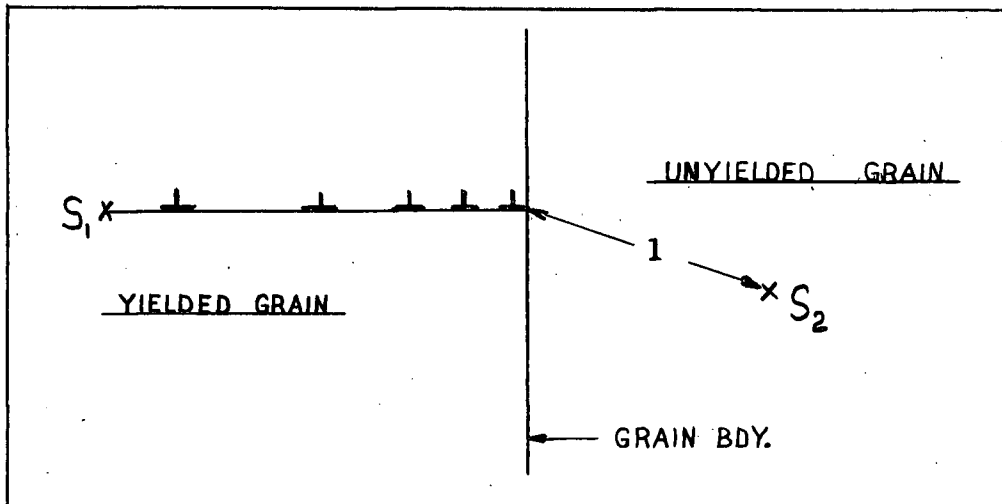


Figure 2. Illustration of grain-to-grain yielding

Yielding will occur when the stress concentration at the next source is

$\sigma_1$ , the unlocking stress, that is

$$\left(\frac{d}{2l}\right)^{1/2} (\sigma_{LY} - \sigma_o) + \sigma_{LY} = \sigma_1, \quad (5)$$

and since  $2l/d \ll 1$ ,

$$\sigma_{LY} = \sigma_o + (2l)^{1/2} (\sigma_1) d^{-1/2} = \sigma_o + k_{LY} d^{+1/2} \quad (6)$$

According to equation (6) and the Cottrell-Bilby theory, the unlocking stress,  $\sigma_1$ , should decrease rapidly with increasing temperature. This would require that  $k_{LY}$  also decreases with temperature which is not generally observed.

The quantity  $\sigma^*$  is known as the thermal component of the flow stress. It arises from short range forces on moving dislocations which can be overcome by thermal activation.

The use of rate theory as a means of studying thermally activated flow became firmly established after the publication of Basinski's classic paper<sup>8</sup> in 1959. His analysis was developed for f. c. c. metals but it is also adaptable to b. c. c. metals.

Various refinements and modifications have since been made to the rate analysis by such workers as Conrad and Wiedersich,<sup>9</sup> Mordike and Haasen<sup>10</sup> and D. P. Gregory<sup>11</sup>.

Let us assume that a dislocation is held up by an obstacle, the nature of which is still not defined. This will create an energy barrier which we can depict by the force-distance curve in Figure 3. To surmount this barrier a dislocation must acquire an energy  $H$  over a length  $L$ . If the distance travelled by the dislocation during activation is  $d$ , the activation volume is defined as

$$v^* = b L d \quad (7)$$

where  $b$  is the Burgers vector.

If the dislocation cannot overcome the barrier with the aid of thermal energy alone it is assumed that  $H$  can be reduced with the aid of an applied stress,  $\tau_a$ , by an amount  $v^* \tau_a$  to a value,  $\Delta Q$ , given by

$$\Delta Q = H - v^* \tau_a \quad (8)$$

Assuming the deformation process is thermally activated one obtains the following Arrhenius type equation for the strain rate,  $\dot{\epsilon}$  :

$$\dot{\epsilon} = A e^{-\Delta Q/kT} \quad (9)$$

where  $A = N \nu \lambda$  (10)

where  $N$  is the number of activation sites per unit volume,  
 $\nu$  is the frequency with which the dislocations "try" the barrier,  
 $\lambda$  is the average strain contributed by a dislocation when it overcomes the barrier.

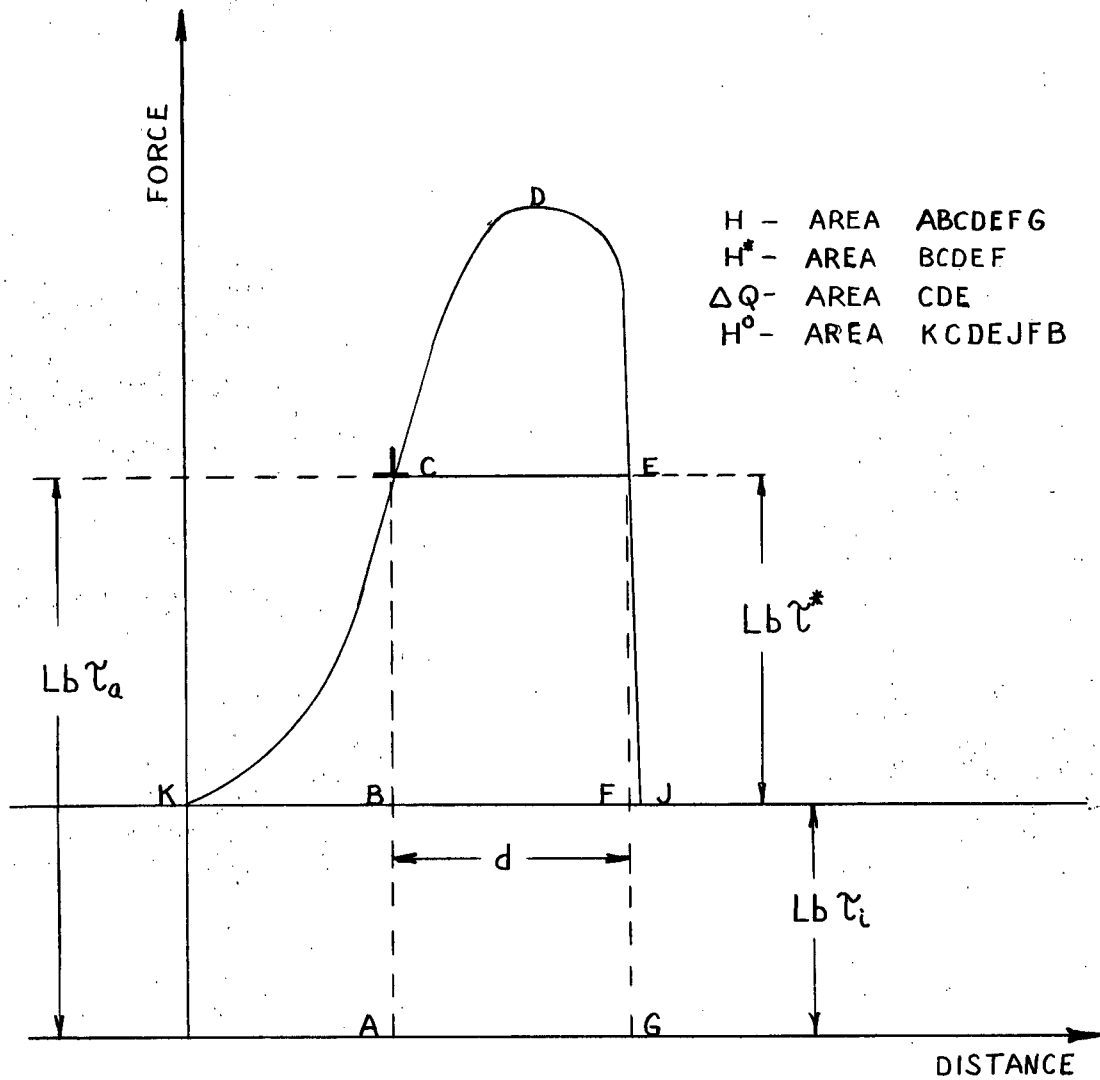


Figure 3. Force-distance curve for thermally activated flow

Gregory remarks that the internal stress field due to a randomly oriented dislocation network should average to zero over long distances but should give rise to a local stress  $\tau_i$  within the dimensions of the network itself. Therefore, the energy,  $H$ , should be made up of two parts given by

$$H = H^* + v^* \tau_i \quad (11)$$

where  $H^*$  is defined in figure (3) and  $v^* \tau_i$  is the energy required to overcome the internal stress field over a distance  $d$ . Substituting equation (11) into equation (8) one obtains

$$\Delta Q = H^* - v^* (\tau_a - \tau_i) = H^* - v^* \tau^* \quad (12)$$

Here  $\tau^*$  is the effective stress operating against the energy barrier. It would be desirable to calculate  $H^*$  directly, for this would yield a good approximate value for the activation energy  $H^0$ . However, there is no direct method of doing this because it requires an evaluation of  $\tau_i$  and therefore, one calculates  $H$  using  $\tau_a$  and estimates  $\tau_i$  by methods of extrapolation.

If the temperature dependence of the shear modulus is neglected and if  $A$  is not a significant function of stress or temperature then the following equations can be derived<sup>11,9</sup>:

$$v^* = k T \left( \frac{\partial \ln \dot{\epsilon}}{\partial \tau_a} \right)_T \quad (13)$$

$$H = v^* \tau_a - v^* T \left( \frac{\partial \tau_a}{\partial T} \right)_{\dot{\epsilon}} \quad (14)$$

$$\Delta Q = k T^2 \frac{\left(\frac{\partial \tau_a}{\partial T}\right) \dot{\epsilon}}{\left(\frac{\partial \tau_a}{\partial \ln \dot{\epsilon}}\right)_T} \quad (15)$$

These equations along with equation (9) provide the means of analysis.

Several workers during the last two or three years have attempted to establish a mechanism for thermally activated flow by comparing measured values of  $v^*$ ,  $H^0$ ,  $\Delta Q$  and  $A$  with theoretically calculated values.

Basinski and Christian<sup>12</sup> observed that the change in flow stress for a change in strain rate decreased with increasing deformation for iron. They concluded that the Peierls-Nabarro force is the dominant factor after ruling out an interstitial mechanism and a forest intersection mechanism. However, they did not consider any other possible mechanisms.

Conrad<sup>14,15,16,19</sup> favours a Peierls mechanism also. He selects this one after ruling out all others on the basis of disagreement between theory and experiment on values of  $H^0$  and  $v^*$ .

Mordike and Haasen<sup>10</sup> favour an impurity mechanism for iron in which finely divided precipitates are responsible for the thermal component of the flow stress. They explain an increase in the strain rate sensitivity of the flow stress with strain in terms of a division of precipitates during straining due to intersection with dislocations. This results in a greater density of obstacles and hence a smaller activation volume.

In another publication, Mordike, referring to his work on tantalum, was unable to determine any definite mechanism although he suggests a mechanism involving the conservative motion of jogs. However, this mechanism, which was first suggested by Hirsch<sup>20</sup> for f.c.c. metals, involves the constriction of extended jogs which are not generally observed in b.c.c. metals.

Gregory et al.<sup>11</sup> favour a mechanism involving the non-conservative motion of jogs for columbium on the grounds that their measured activation energy was too high to be compatible with any other mechanism.

A summary of the previous work is given in Table I.

TABLE I

Author	Material	H <sup>0</sup> (ev)	L (cm)	Mechanism	Ref.
Conrad	Fe	.5-.6	30 b	Peierls	14
Basinski + Christian	Fe	Did not Calculate	Did not Calculate	Peierls	12
Conrad + Frederick	Fe	Did not Calculate	12 b	Peierls	19
Mordike + Haasen	Fe	.5	17 b	Impurity Mechanism	10
Mordike	Ta	1.3	55 b	Conservative jog mech. (not definite)	13
Gregory et al	Cb	2	50 b	Non conservative jog.	11

## II. EXPERIMENTAL

### A. Material

The vanadium for this project was supplied by Union Carbide Canada Limited, of Toronto, Ontario. It was in the form of cylindrical polycrystalline rods 0.250 inches in diameter. The results of an analysis for interstitial gases and carbon are given in Table II.

TABLE II

Analysis of Material

Impurity	"As Received" (p.p.m)	Zone Refined (p.p.m.)
Oxygen	680	160
Carbon	314	136
Nitrogen	259	318
Hydrogen	8.9	7.2

## B. Zone Refining

Single crystals were grown in the electron beam floating zone refiner described by Snowball<sup>17</sup>.

"As-received" rods were used in nine inch lengths. A portion of one end, roughly 0.75 inches in length, was machined down to a diameter of 0.125 inches to fit the lower grip on the zone refiner. The other end was faced off squarely in a lathe.

A seed crystal, about one inch in length, was prepared in a similar fashion and fitted to the upper grip of the zone refiner such that there was a gap of approximately 1/16" between the seed and the rod. The filament was lined up so that it was just above the gap and the power was turned on.

It was found necessary to use a current of 130 ma. and a potential difference of 1.6 kV. to maintain a stable molten zone. Minor adjustments were necessary during the pass due to fluctuations in the power supply, gas bursts from the rod and other minor effects.

Two passes were given to each rod. The first pass was done at 25 cm. per hour and was primarily intended to outgas the specimen. The second pass was intended to purify the rod and was carried out at 10 cm per hour.

The vacuum maintained was generally better than  $10^{-5}$  mm of Hg.

An analysis for interstitials in zone refined material is given in Table II.

## C. Specimen Preparation

### 1. Machining

Polycrystalline and single crystal specimens were both prepared for testing by the same procedure. The polycrystalline specimens were manufactured from "as-received" rod.

A 1 1/4" length was cut from a rod and machined down to a diameter of from .110" to .130" with a gauge length of about one inch. The initial cuts were .003" deep. At a diameter of about .150" the depth was reduced after every four cuts to .002", .001" and .0005". The specimen was then hand polished in the lathe with 0 and 000 emery paper.

### 2. Electropolishing

To remove any surface deformation, all specimens were electropolished in a solution of the following composition:

320 cc methyl alcohol,  
80 cc conc. sulfuric acid.

The polishing was carried out at room temperature with a potential difference of about 10 volts and a current of 1.5 amperes. In all cases a minimum of .005" was removed from the surface of the specimen. This required a polishing time of from fifteen to twenty minutes.

### 3. Grain Size Determination and Control

Grain size was controlled by heat treatment in the vacuum annealing furnace described by Fraser<sup>18</sup>. The vacuum was generally kept well below  $10^{-5}$  mm of Hg. A table of temperatures, times and resultant grain sizes is given in Appendix I.

Samples were cut from the annealed specimens, mounted and polished for metallographic examination. The polished specimens were etched in a solution of

15 cc. conc. lactic acid,  
15 cc. conc. nitric acid,  
2-3 cc. conc. hydrofluoric acid,

and photomicrographs were taken.

The mean grain diameter was determined by the intercept method. Six lines were drawn across the photograph as in Figure 4. The number of grain boundaries cutting each line was counted and, knowing the magnification, the mean grain diameter was calculated.

#### D. Tensile Testing

Specimens were tested on an Instron tensile testing machine. The mounting device consisted of the set of universal grip holders described by Snowball<sup>17</sup> and a set of grips designed specifically for the type of specimen used. A diagram of the grips is shown in Figure 5.

Three types of tensile tests were performed:

- (1) Continuous tests on polycrystals.
- (2) Strain rate change tests on single crystals and polycrystals.
- (3) Temperature change tests on single crystals and polycrystals.

In the continuous tests the specimens were strained continuously to fracture at a constant rate of crosshead travel of .02 inches per minute.

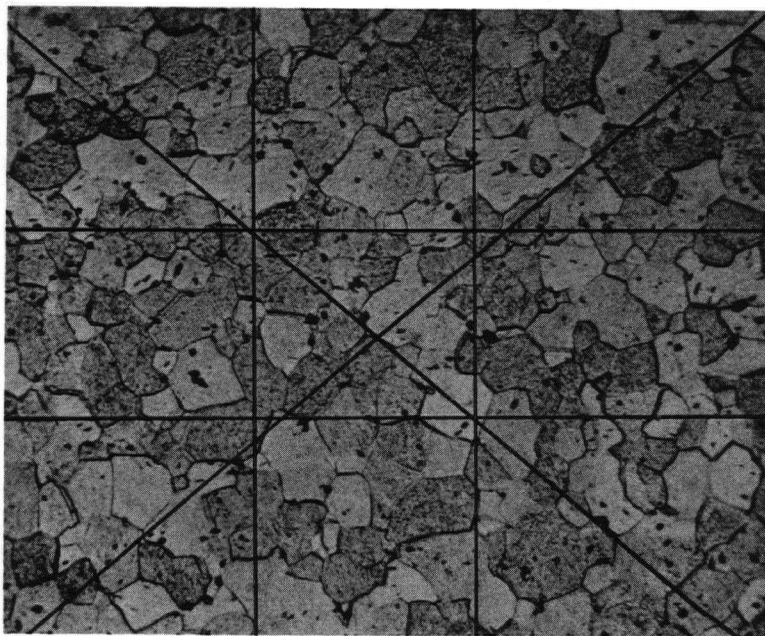


Figure 4. Method of grain size measurement, specimen 9B, 210X.

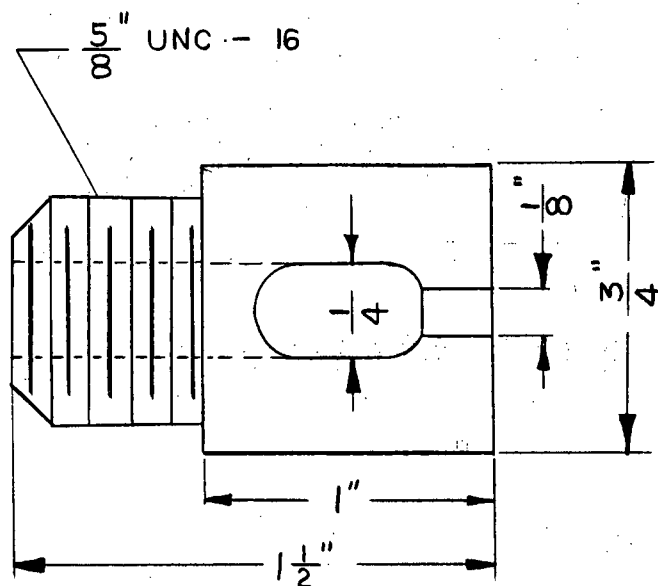


Figure 5. Drawing of grips used in tensile testing.

In the strain rate change tests the specimens were strained past initial yielding until the specimen began to work harden. Then the crosshead was stopped and the load relaxed, usually to about eighty percent of the flow stress. The crosshead speed was increased by a factor of ten or one hundred and the straining was resumed for another 0.5% strain. Then the crosshead was stopped, the load was relaxed and the crosshead was restarted at the initial strain rate. This cycling process was continued until the specimen failed. These experiments were carried out over a temperature range of  $-72^{\circ}\text{C}$  to  $100^{\circ}\text{C}$ .

The strain rates employed here were mainly those corresponding to a crosshead speed of .01 inches per minute for the basic rate with increases of 10 or 100 times.

The temperature change tests were similar except that the temperature was cycled at a constant strain rate. This involved straining past the yield point up to a given strain at one temperature, stopping the crosshead, relaxing the load, changing the temperature bath and reloading at the same strain rate after allowing time for thermal equilibrium to be reached. This cycling process was continued until the specimen failed.

#### E. Temperature Control

Three principal temperature baths were used. A boiling water bath was used to maintain a temperature of  $100^{\circ}\text{C}$ . A photograph of this assembly is shown in Figure 6.

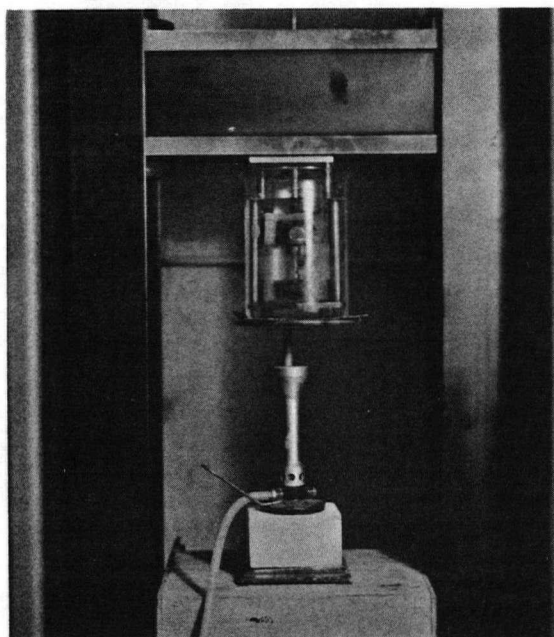


Figure 6. Assembly for testing at  $100^{\circ}\text{C}$ .

An ice water bath was used to obtain a temperature of  $0^{\circ}\text{C}$  and a mixture of acetone and solid  $\text{CO}_2$  provided a temperature bath of  $-72^{\circ}\text{C}$ .

A salt bath of calcium chloride and ice water was used for two tests on single crystals but it was inconvenient to use and was not employed in further tests.

The temperatures of the water baths were measured with a mercury-in-glass thermometer. The temperatures of the low temperature baths were measured with a copper-constantan thermocouple.

### III. EXPERIMENTAL RESULTS

#### A. Polycrystalline Material

##### 1. Grain Growth

Using the annealing procedures outlined in the introduction, a set of specimens was obtained with mean grain diameters ranging from 15 microns to 90 microns.

Initially, attempts were made to obtain polycrystals of higher purity by zone refining the "as-received" material. This process yielded a single crystal and attempts were made to make polycrystals of controlled grain size by wire-drawing and annealing processes.

Two zone refined bars were machined to a constant diameter and drawn down to 50% and 30% of the original cross sectional areas. After annealing, the grain size was small at the periphery and large near the center of the rod, owing to the inhomogeneity of deformation by drawing. A typical structure is shown in Figure (7). Because of the non-uniformity, this procedure was abandoned and specimens were made from "as received" material.

A Laué back-reflection photograph did not reveal any preferred orientation.

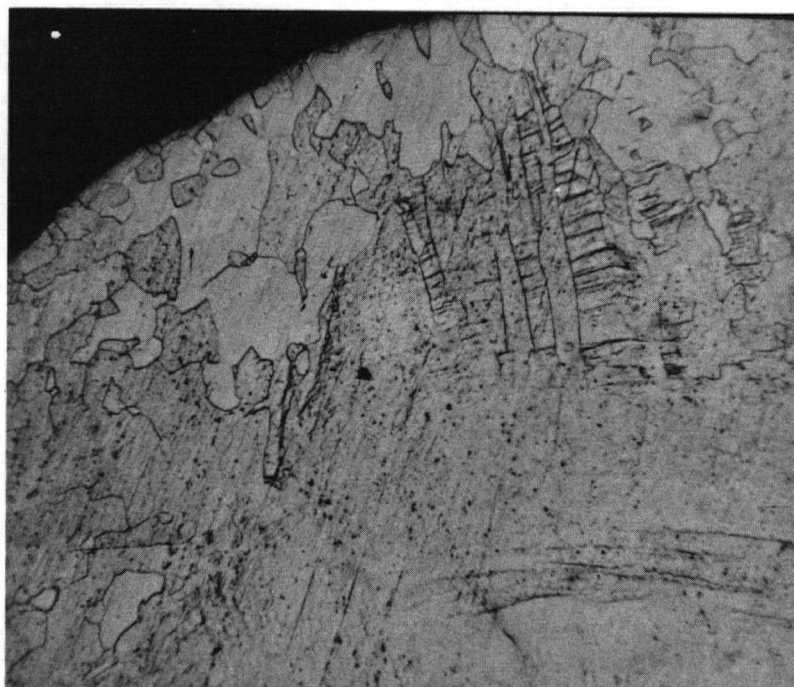


Figure 7. Inhomogeneous grain sizes after drawing, rod #2, 110X.

## 2. Hall-Petch Equation

A typical load-elongation curve for a continuous test on a polycrystal is shown in Figure (8). This diagram also illustrates the method of obtaining the parameters  $\sigma_{f1}$  and  $\sigma_{LY}$ .

Figure (9a) shows the behavior of  $\sigma_{LY}$  and  $\sigma_{f1}$  with respect to  $d^{-1/2}$ . By comparing the two plots it is difficult to see the relationship between  $\sigma_{f1}$  and  $\sigma_{LY}$  because of the scatter. It is more enlightening to study

$$\sigma_{f1} - \sigma_{LY} = (\sigma_o - \sigma_o^o) + (k_{f1} - k_{LY}) d^{-1/2} \quad (16)$$

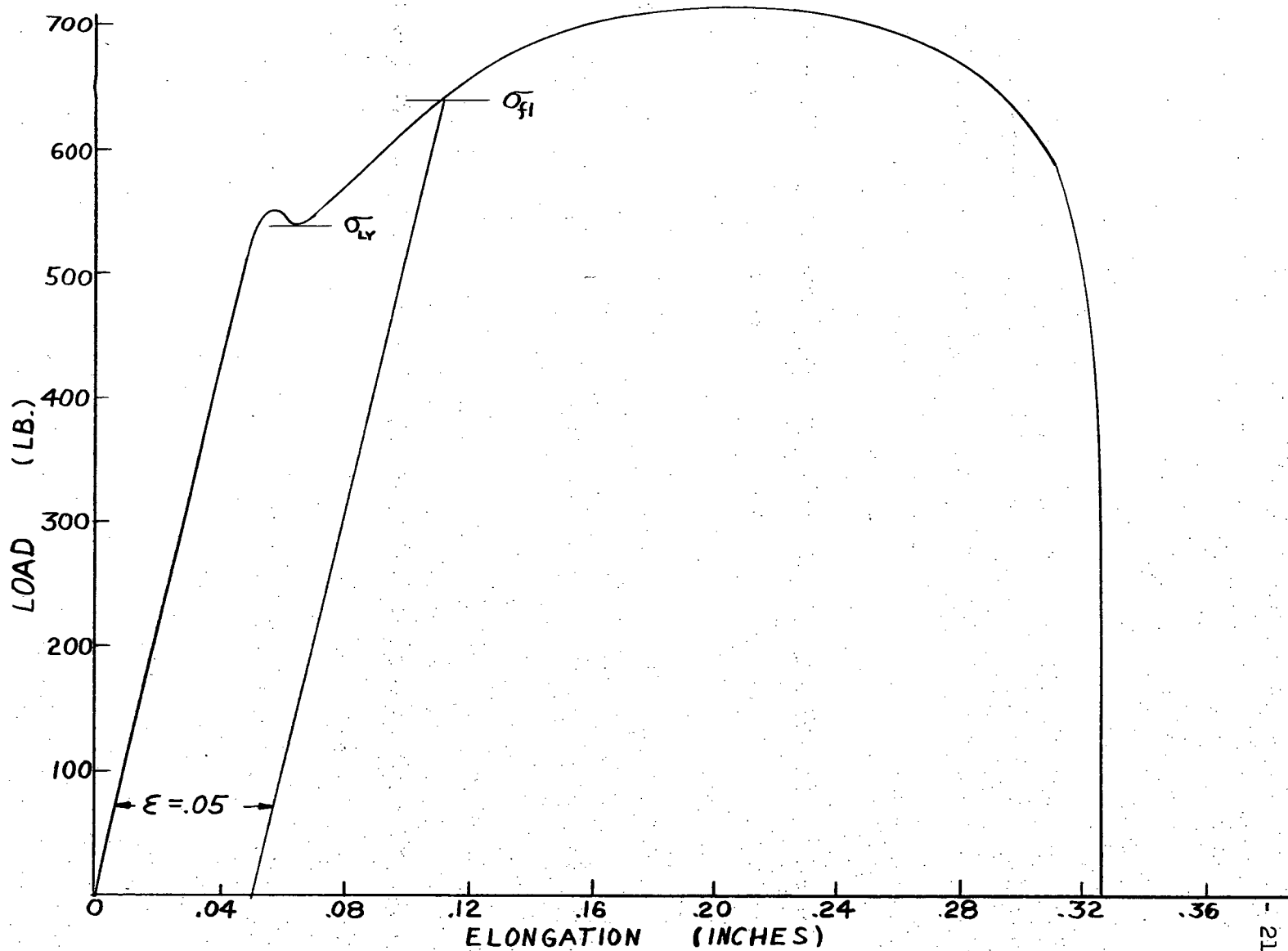


Figure 8. Typical load-elongation curve for vanadium polycrystal.

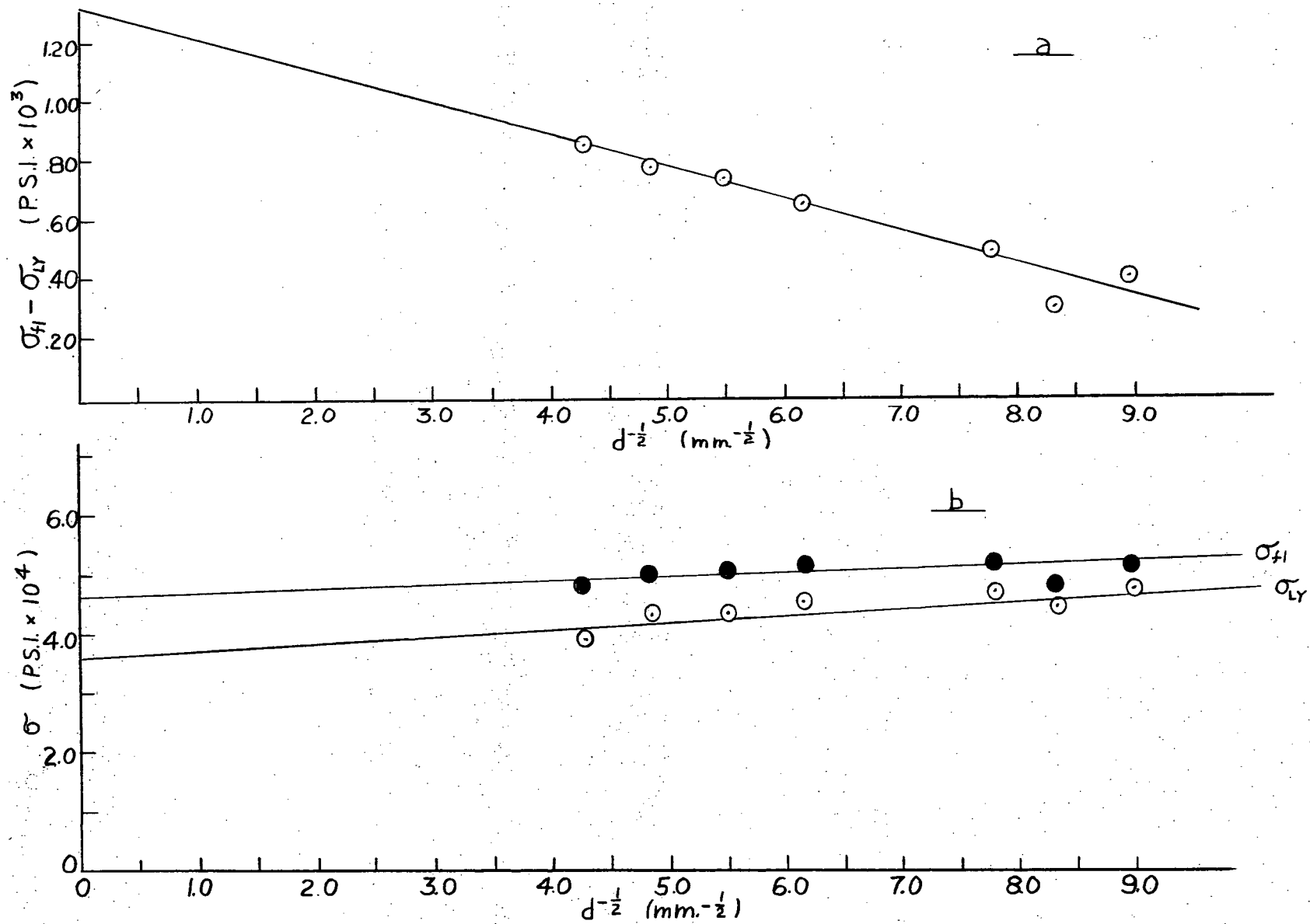


Figure 9. Dependence of yield stress and flow stress on grain size at 25°C.

It is evident that if  $k_{LY} = k_{f1}$  then  $\sigma_{f1} - \sigma_{LY}$  will be a constant, independent of grain size. From Figure (9b) it is evident that  $k_{LY} \neq k_{f1}$ .

$\sigma_{f1} - \sigma_{LY}$  decreases with decreasing grain size. This method of plotting the differences is the most accurate one because the maximum error in these results lies in the measurement of  $d^{-1/2}$ . A comparison of the difference between the yield and flow stresses for a given grain size is independent of the measurement of the grain size.

It would have been desirable to investigate this property further but this would have required testing a large number of specimens to fracture at a constant strain rate. Because of the high cost of vanadium, it was decided to perform only tests which gave a maximum amount of information from each specimen.

All subsequent tests on polycrystals were of the strain rate change or temperature change type. This made it impossible to obtain consistent flow stress values at 5% strain because the deformation history varied from specimen to specimen.

The lower yield stress was measured during all of these tests, however, and is plotted in Figure (10).

There is a trend for the slopes of the plots in Figure (10) to increase with temperature. One might question this trend on the grounds of the uncertainty of grain size measurement. However, the specimens of various grain sizes were made in batches and a specimen from each batch was tested at each temperature. The grain size was measured and a single value was allotted to each batch. Therefore, if there was an error in the

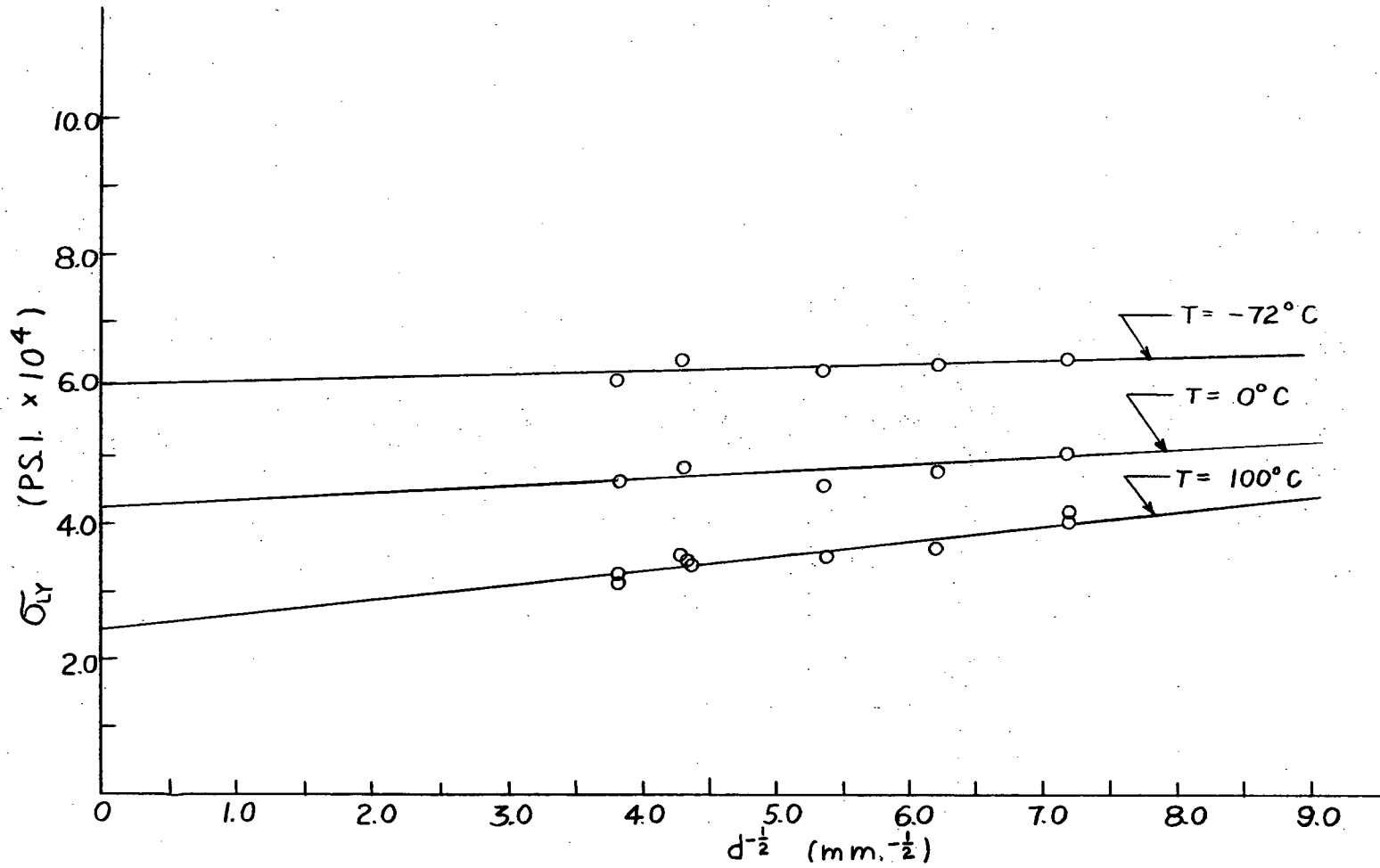


Figure 10. Dependence of lower yield stress on grain size.

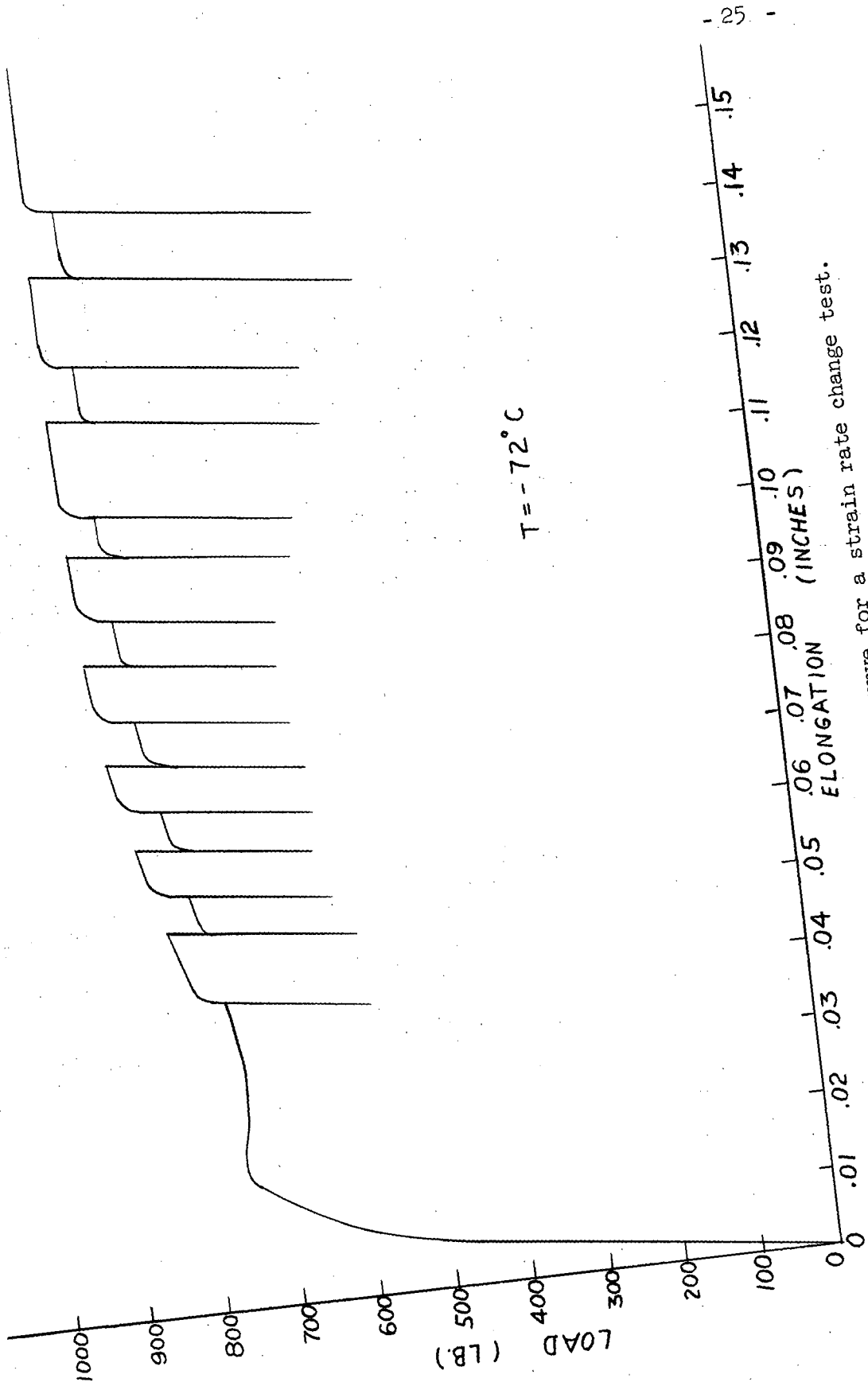


Figure 11. Typical load-elongation curve for a strain rate change test.

grain size measurement it would be the same for all the specimens of the given batch, and the relative slopes of the curves would not be affected.

### 3. Strain Rate Change Tests

A typical stress-strain curve involving strain rate changes is shown in Figure (11). The stress level at the initiation of plastic flow was found by extrapolating the two straight portions of the curve in Figure (12) and calculating the strain rate sensitivity  $\Delta \sigma$  from the equation

$$\Delta \sigma = \sigma(B) - \sigma(A). \quad (17)$$

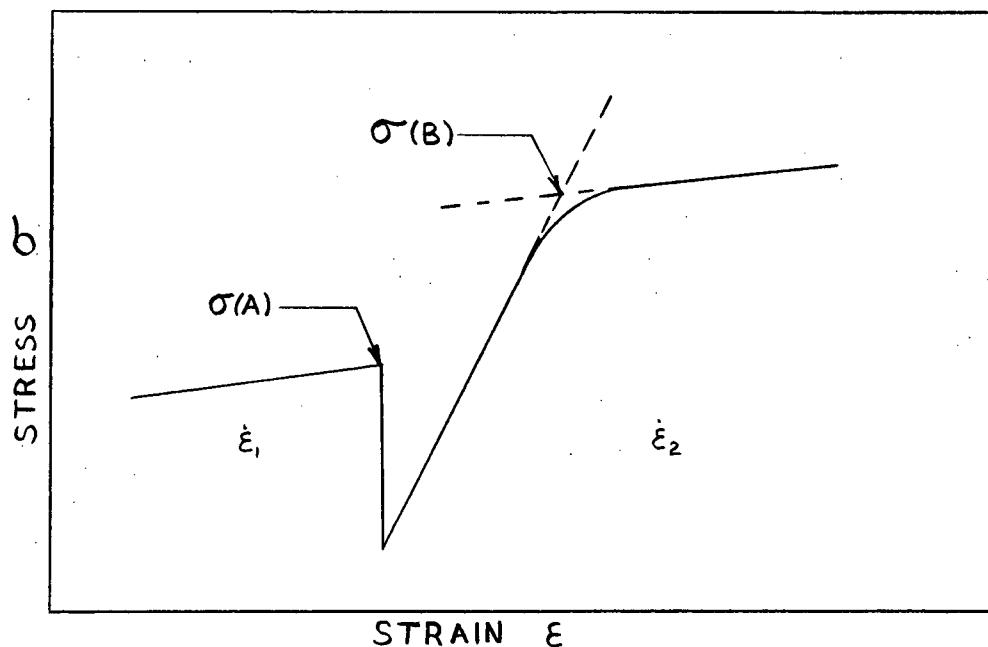


Figure 12. Method of extrapolation to obtain change in flow stress

$\Delta \tau_a$ , the change in the resolved shear stress, was calculated assuming a Schmid factor of 0.5.  $\Delta \tau_a$  was then plotted as a function of  $\tau_a$  and  $\epsilon$  in Figures (13), (14) and (15). The general trend in these plots is for  $\Delta \tau_a$  to decrease slightly with deformation in disagreement with the Cottrell-Stokes Law.

It is evident that there is no measureable dependence of  $\Delta \tau_a$  on grain size over the range studied. This is in agreement with the work of Conrad and Schoeck on polycrystalline iron.

Temperature, in the range studied, has no measureable effect on the slopes of the plots in Figures (13), (14) and (15). However, one test at room temperature yielded a zero slope which suggests that the scatter in these types of measurements is sufficient to mask a small temperature dependence of the slope.

#### 4. Temperature Change Tests

A series of temperature change tests was performed on the polycrystalline material between 100°C and 8°C. The reason for using 8°C was one of convenience. It was found that upon removal of the boiling water bath and switching to an ice water bath the assembly and bath came to temporary thermal equilibrium at about 8°C. The variability of this process was rarely more than  $\pm 1^\circ\text{C}$  and it was easier to adjust the bath temperature to 8°C than to cool the system to 0°C.

The specimen was allowed at least ten minutes to attain the bath temperature at 8°C and at least five minutes at 100°C. The shorter time was considered sufficient for the high temperature because the heating

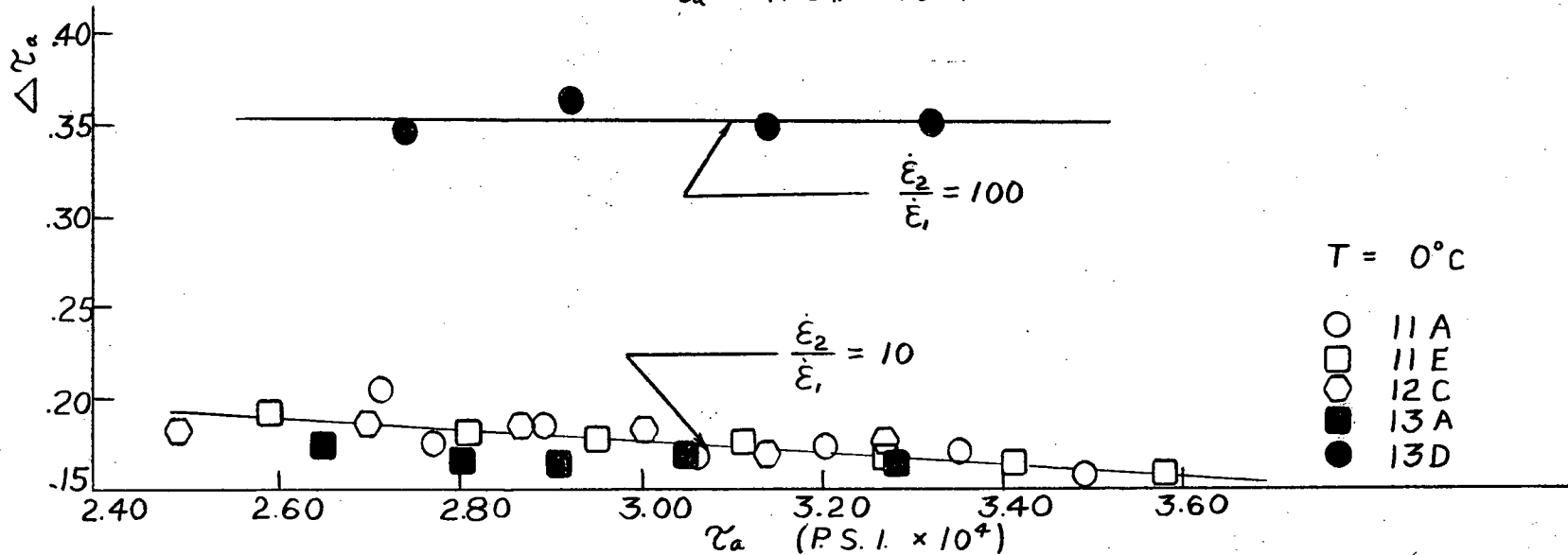
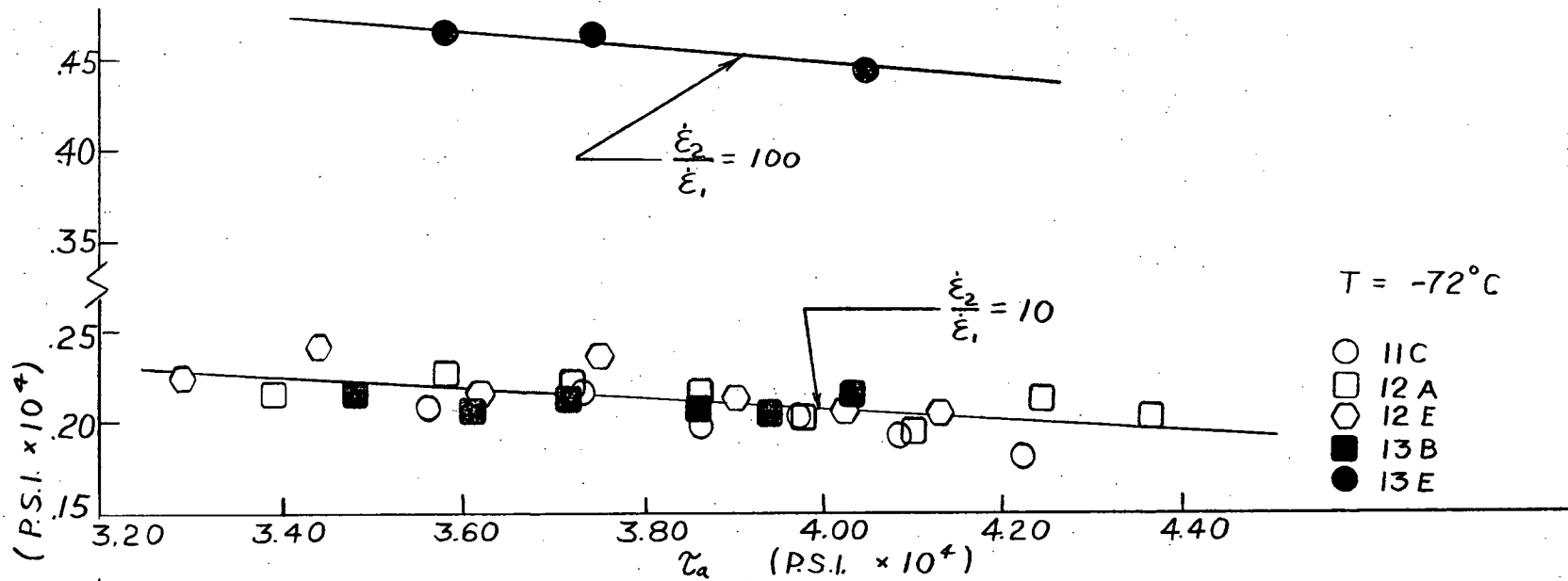


Figure 13.  $\Delta\tau_a$  for an increase in  $\dot{\epsilon}$  vs.  $\tau_a$  for polycrystals.

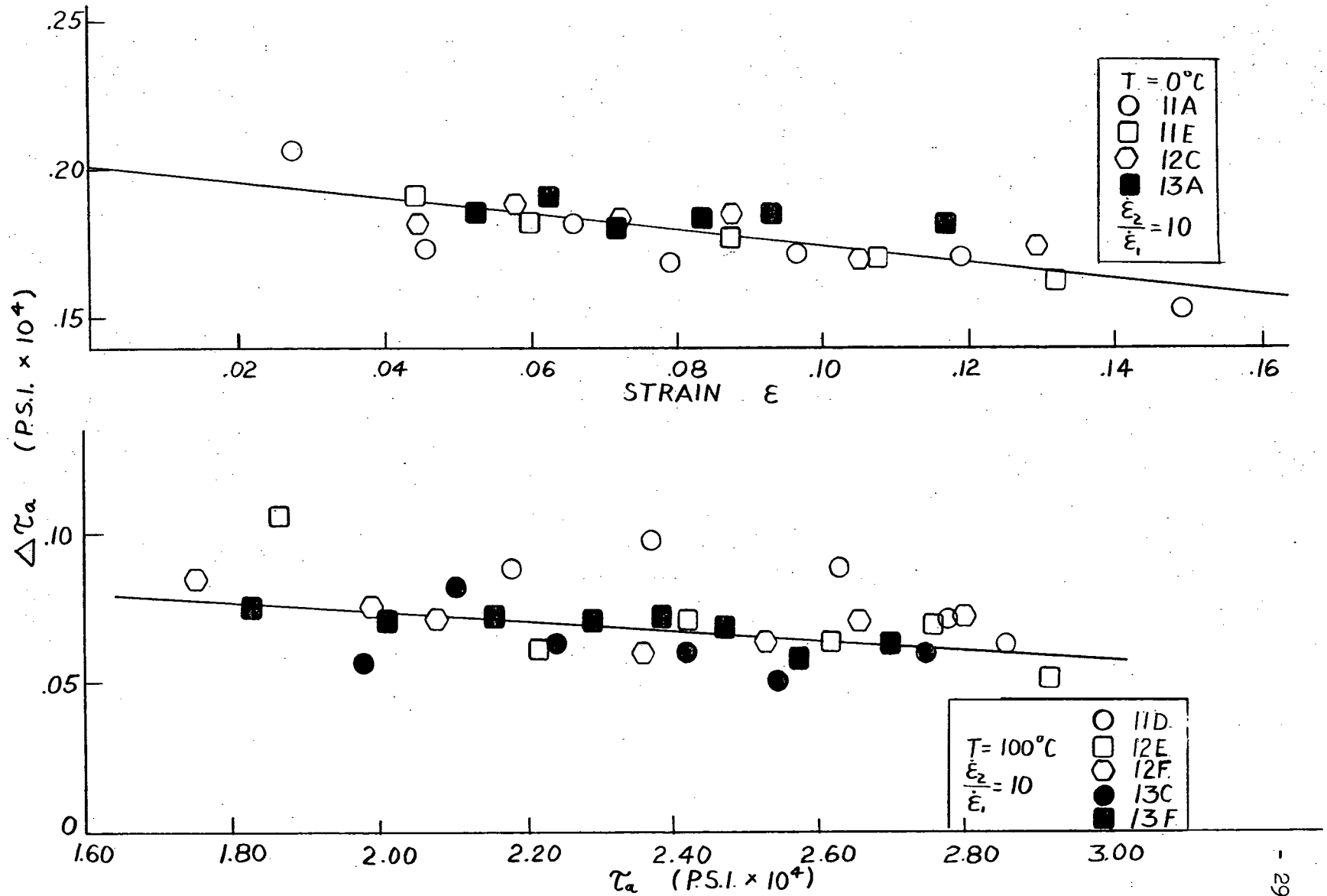


Figure 14.  $\Delta\tau_a$  for an increase in  $\dot{\epsilon}$  vs.  $\tau_a$  and  $\epsilon$  for polycrystals.

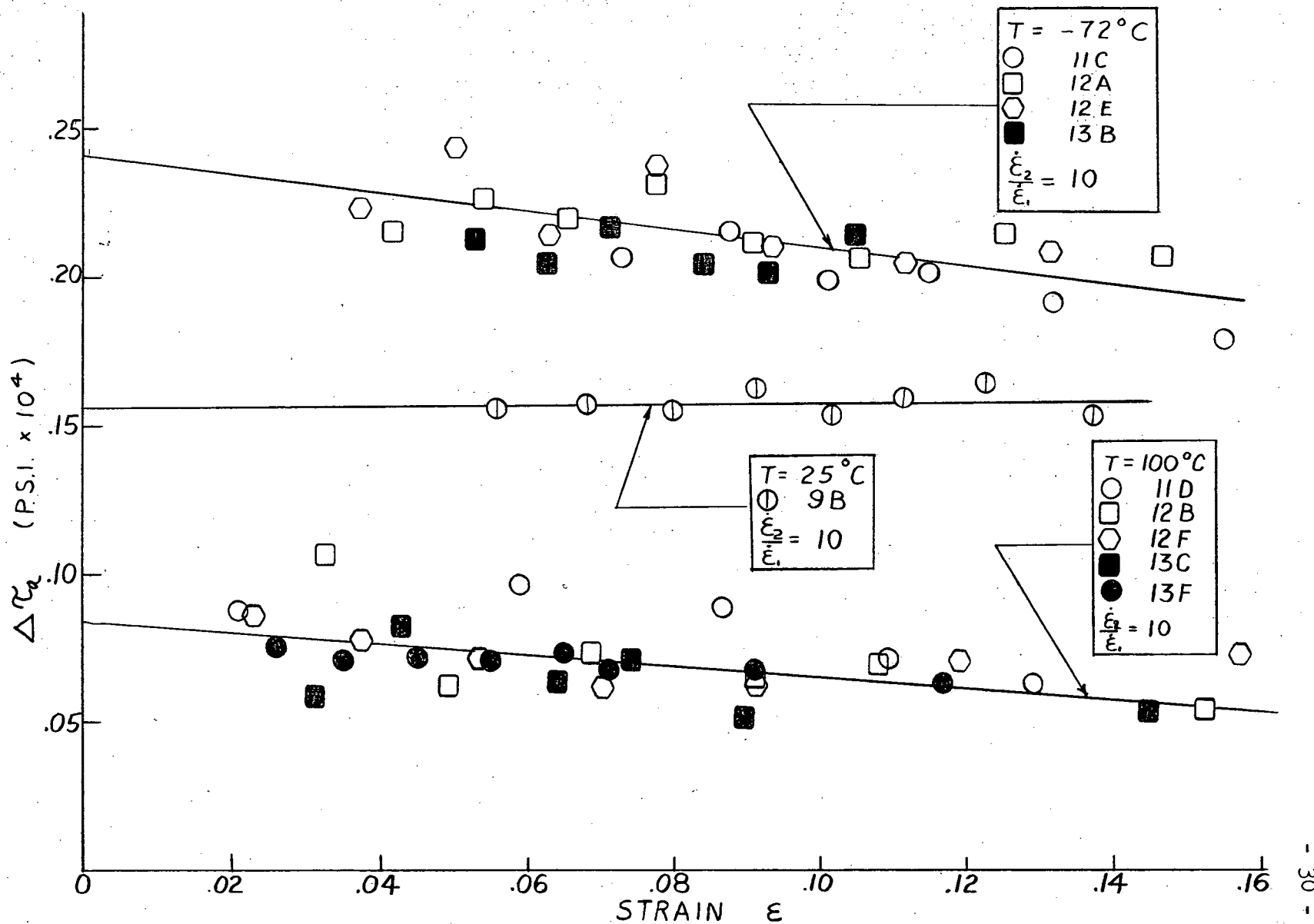


Figure 15.  $\Delta\tau_a$  for an increase in strain rate vs  $\epsilon$  for polycrystals.

process was slow. This made it unlikely that the specimen was ever more than a few degrees below the bath temperature.

Plots of  $\Delta \tau_a$  against  $\tau_a$  and  $\epsilon$  are shown in Figure (16). The trend here is for  $\Delta \tau_a$  to decrease with increasing stress and strain. It is notable that the magnitude of  $\Delta \tau_a$  is roughly twice that for a strain rate change of a factor of ten at  $0^\circ\text{C}$ . Therefore, there would be a greater likelihood of detecting a grain size sensitivity of  $\Delta \tau_a$  in these tests. However, such a sensitivity is not observed.

#### 5. "Pseudo" Yield Points

Under certain conditions yield points were observed upon reloading the specimen after a strain rate or temperature change. A typical stress-strain curve showing this property is included in Figure (17). These yield points were observed under the following conditions:

- (1) In strain rate change tests at  $100^\circ\text{C}$ ,
- (2) In temperature change tests involving  $100^\circ\text{C}$ .

In the temperature change tests the yield drop was observed on both the low temperature and the high temperature portions of the stress-strain curve, but the yield drops were slightly larger on the former portion. The magnitude of the yield drops was roughly the same for both the upper and lower strain rates in the rate change tests. The size of these yield drops was in all cases independent of strain. Because of the temperature dependence of the yield drops it is unlikely that they could be due to any characteristic of the testing apparatus.

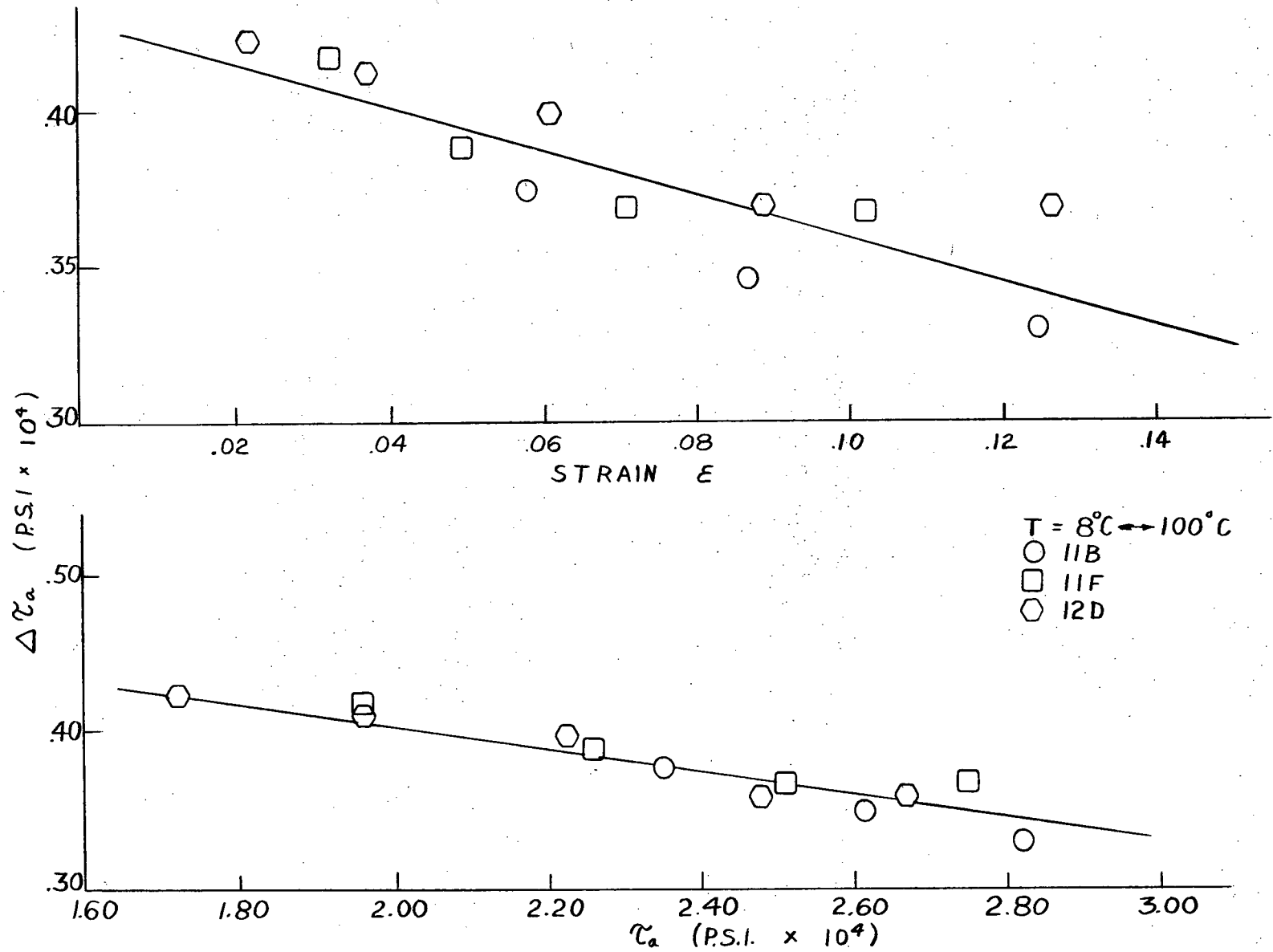


Figure 16.  $\Delta\tau_a$  for a decrease in temperature vs.  $\epsilon$  and  $\tau_a$  for polycrystals.

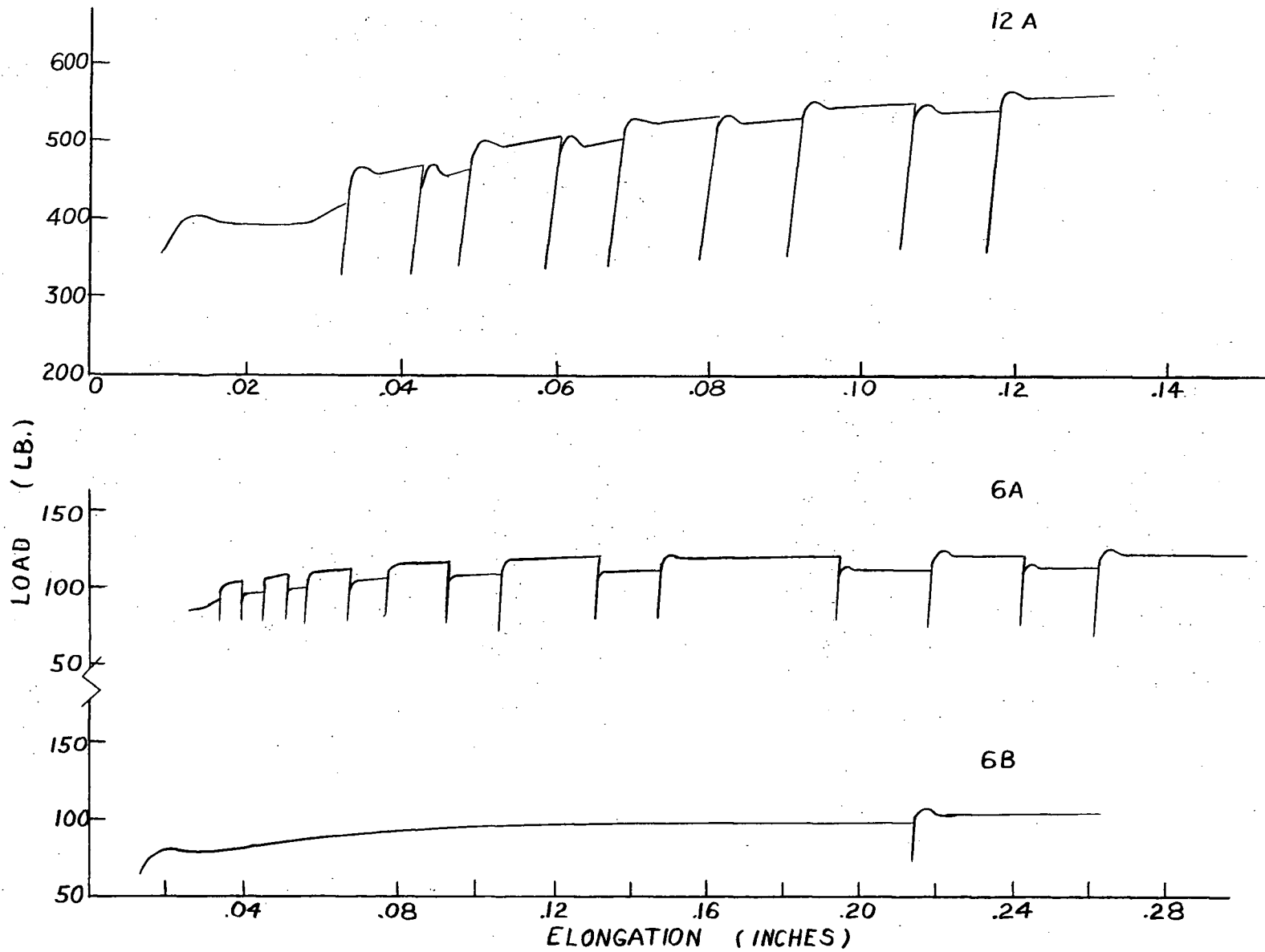


Figure 17. Load-elongation curves showing yield points.

The occurrence of these yield points created the problem of how to measure the flow stress upon reloading. For reasons discussed later the method of extrapolation illustrated in Figure (18) was used.

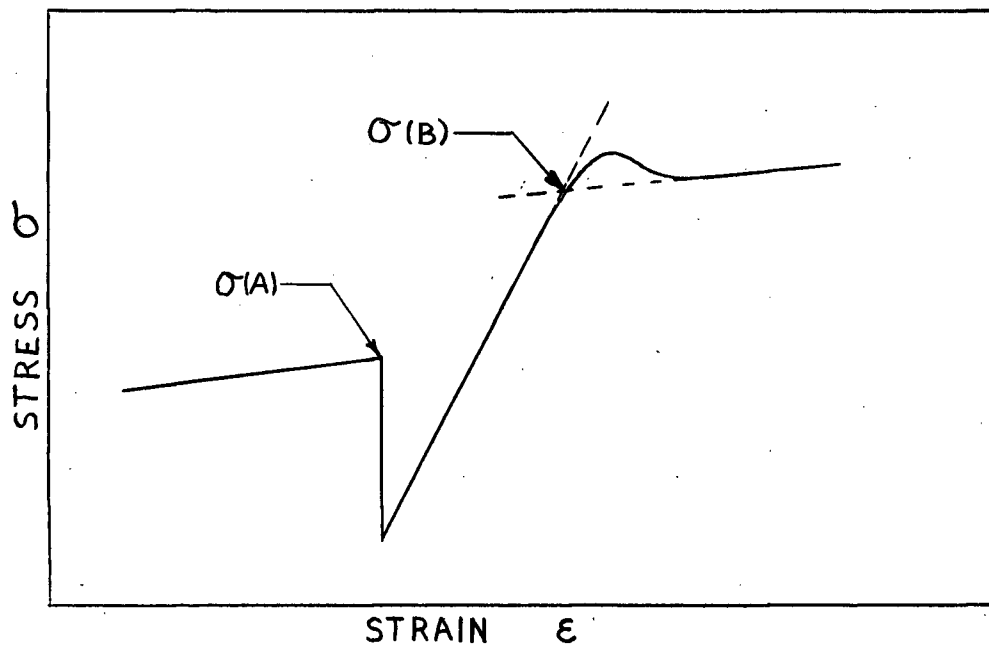


Figure 18. Method of extrapolation through yield points.

## 6. Rate Equation

The activation volume was calculated for each specimen and plotted as a function of stress. To do this, the strain rate sensitivity was found from the points in Figures (13) and (14) and used in equation (13).

Results of these calculations are plotted in Figure (19). There appears to be a slight increase in  $v^*$  with stress at  $0^\circ\text{C}$  and  $-72^\circ\text{C}$ . This increase is small, however, and therefore an average value of  $v^*$  was taken and plotted against temperature. This is shown in Figure (20).

The energy,  $H$ , was calculated using data from the temperature change tests and equation (14). The value of  $v^*$  used in this equation was that for the mean temperature of the test,  $327^\circ\text{K}$ . Since no strain rate change test was done at  $327^\circ\text{K}$ ,  $v^*$  was found by interpolation on Figure (20).  $H$  is plotted as a function of strain in Figure (21). It is seen that  $H$  increases somewhat with strain.

Using equation (15), the thermally activated component of the activation energy,  $\Delta Q$ , was calculated for a temperature of  $327^\circ\text{K}$  and at 10% strain. The value obtained was .60 e.v.  $\Delta Q$  was also calculated from equation (8) and plotted as a function of strain in Figure (22). The value for  $\tau_a$  in this equation was taken as the average of the applied stresses at the two testing temperatures. From Figure (22),  $\Delta Q$  at 10% strain is 0.72 e.v. This is somewhat different from the value obtained in equation (15) and serves as a rough measure of the accuracy of this type of analysis.

The factor  $A$  in the rate equation was determined from equation (9) and is plotted in Figure (23) as a function of strain.

A rough estimate of the activation energy,  $H^\circ$ , may be made with the aid of Figure (24a). When the strain rate sensitivity is equal to zero

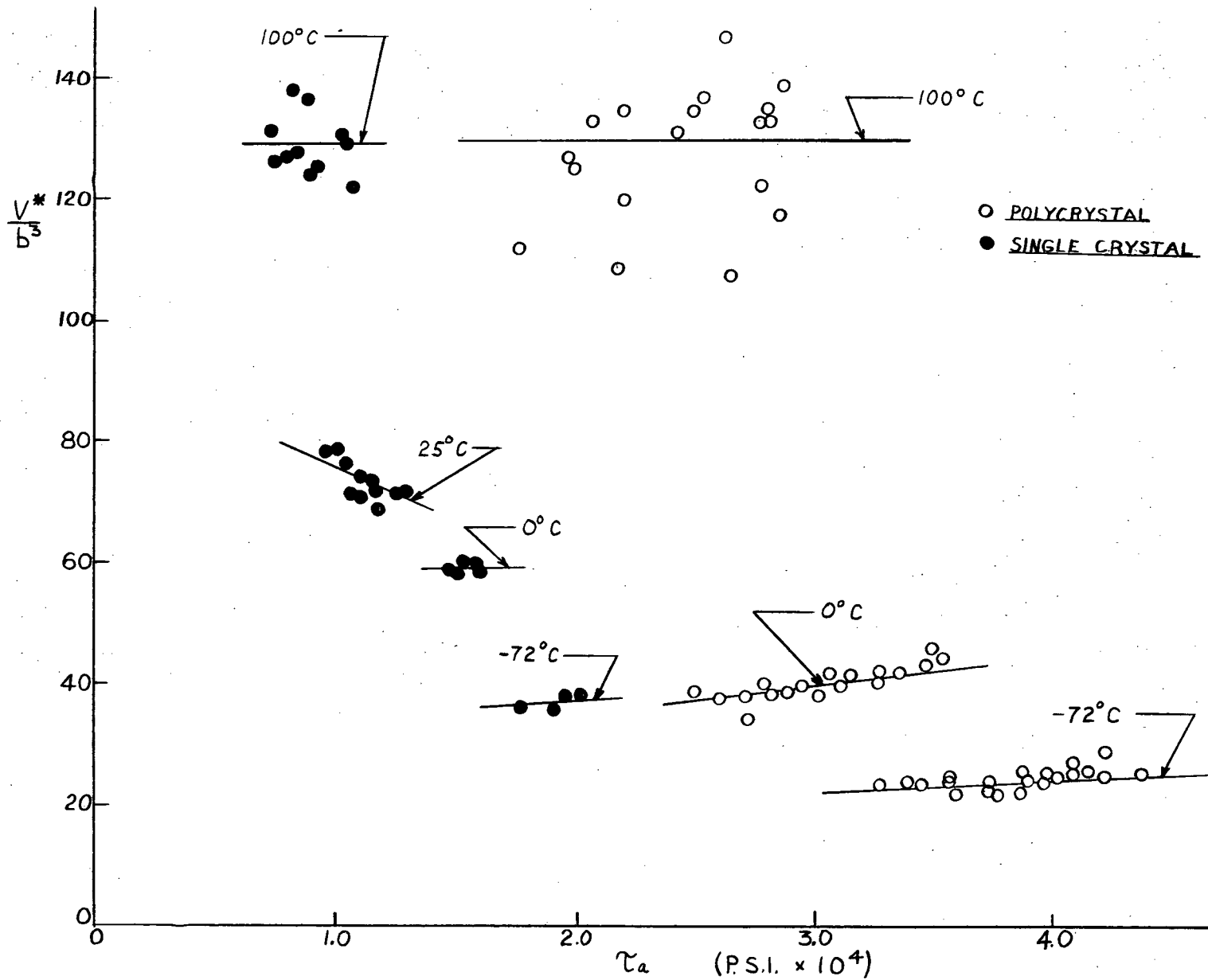


Figure 19. Activation volume vs. flow stress

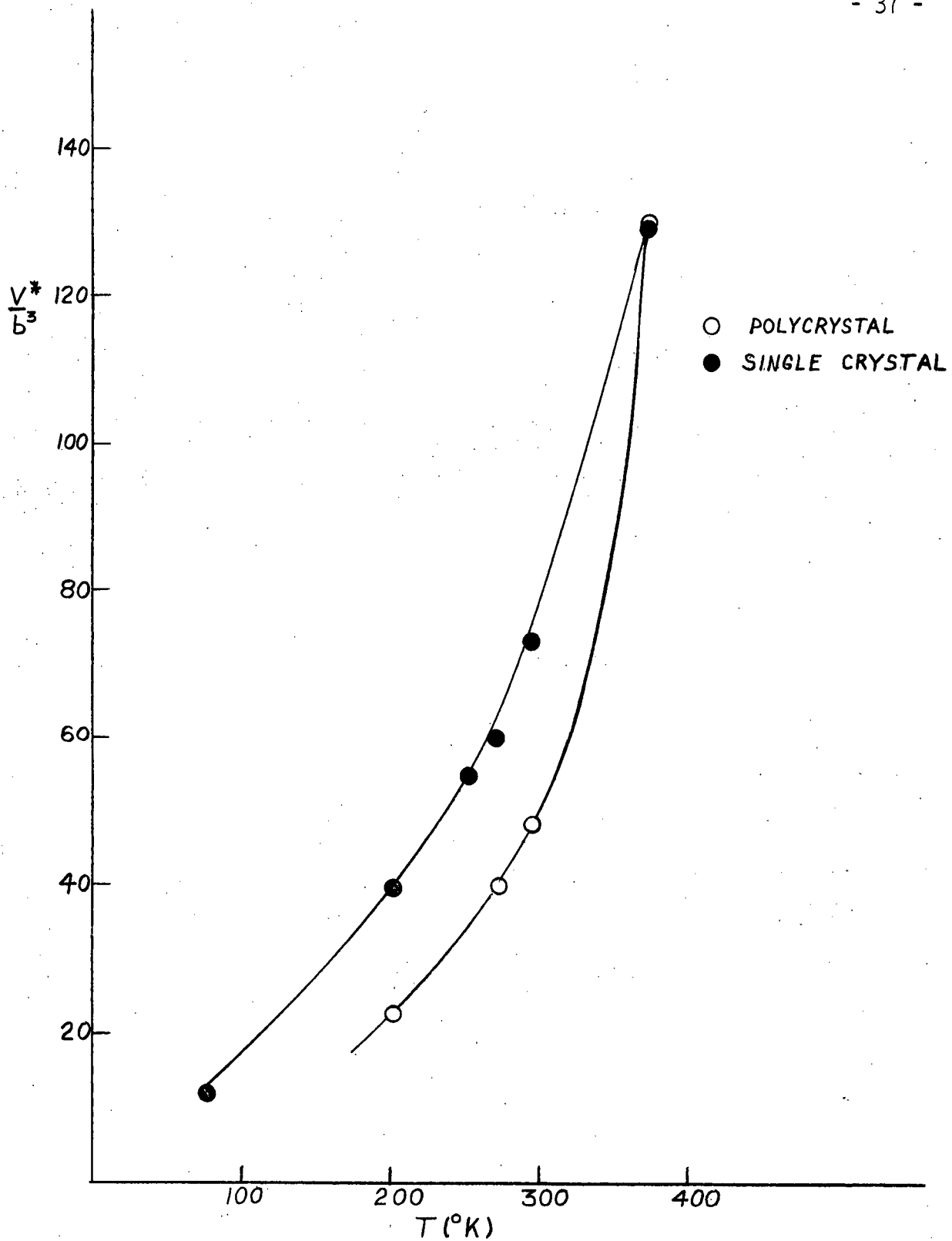


Figure 20. Activation volume vs. temperature.

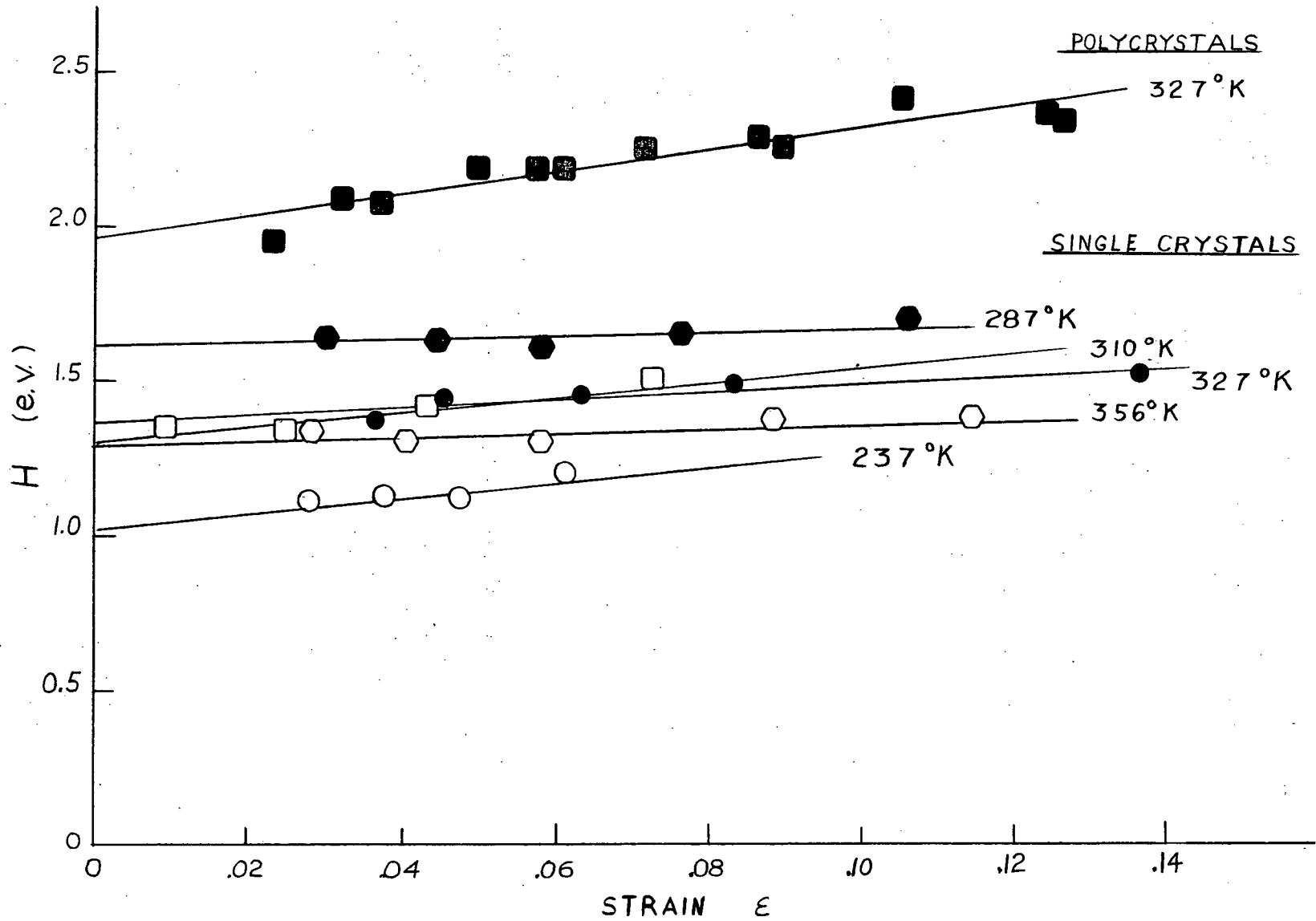


Figure 21. Energy,  $H$ , vs.  $\epsilon$

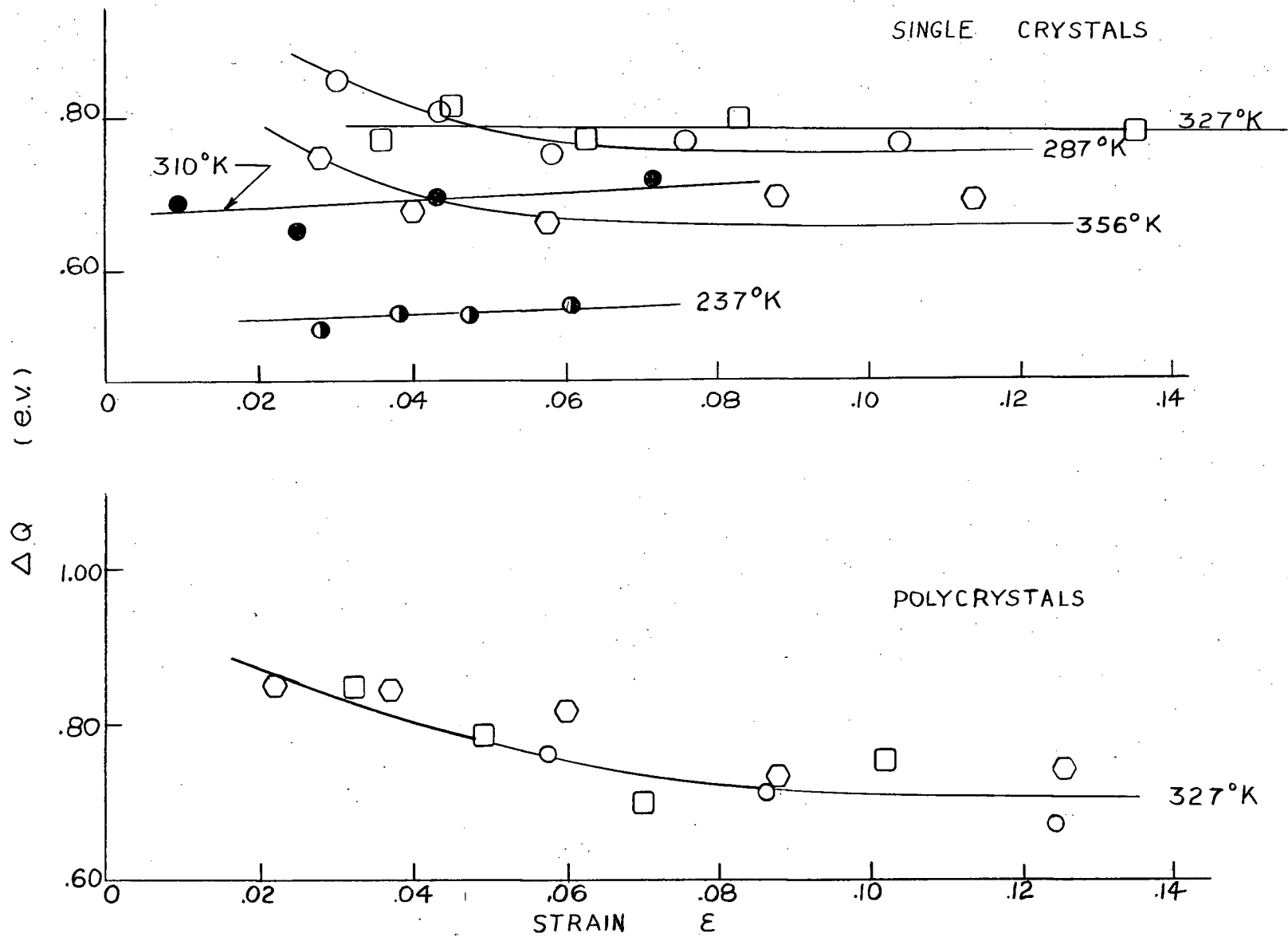


Figure 22. Thermally activated component of  $H^0$ ,  $\Delta Q$ , vs.  $\epsilon$ .

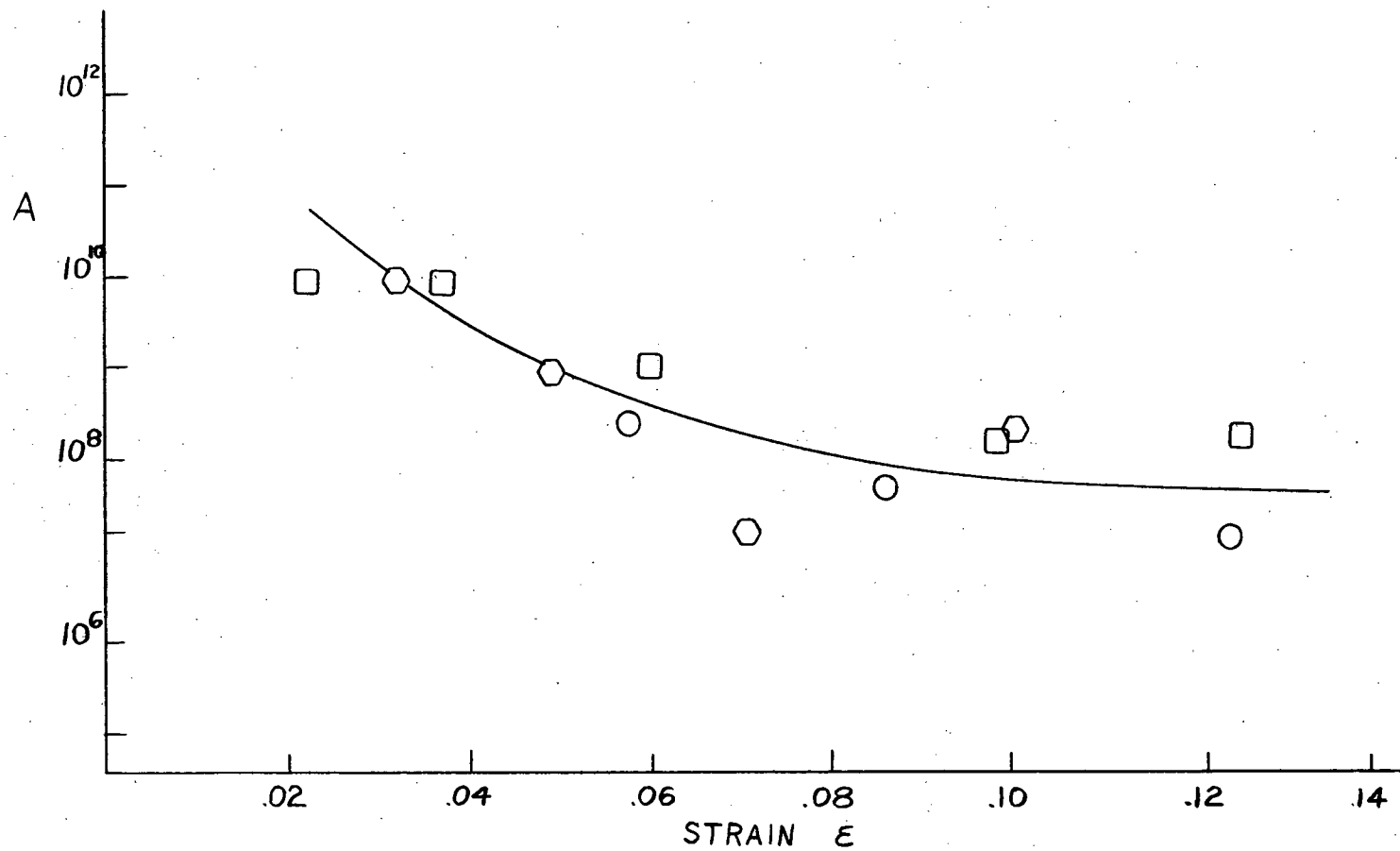


Figure 23. Pre-exponential factor  $A$  vs.  $\epsilon$  for polycrystals.

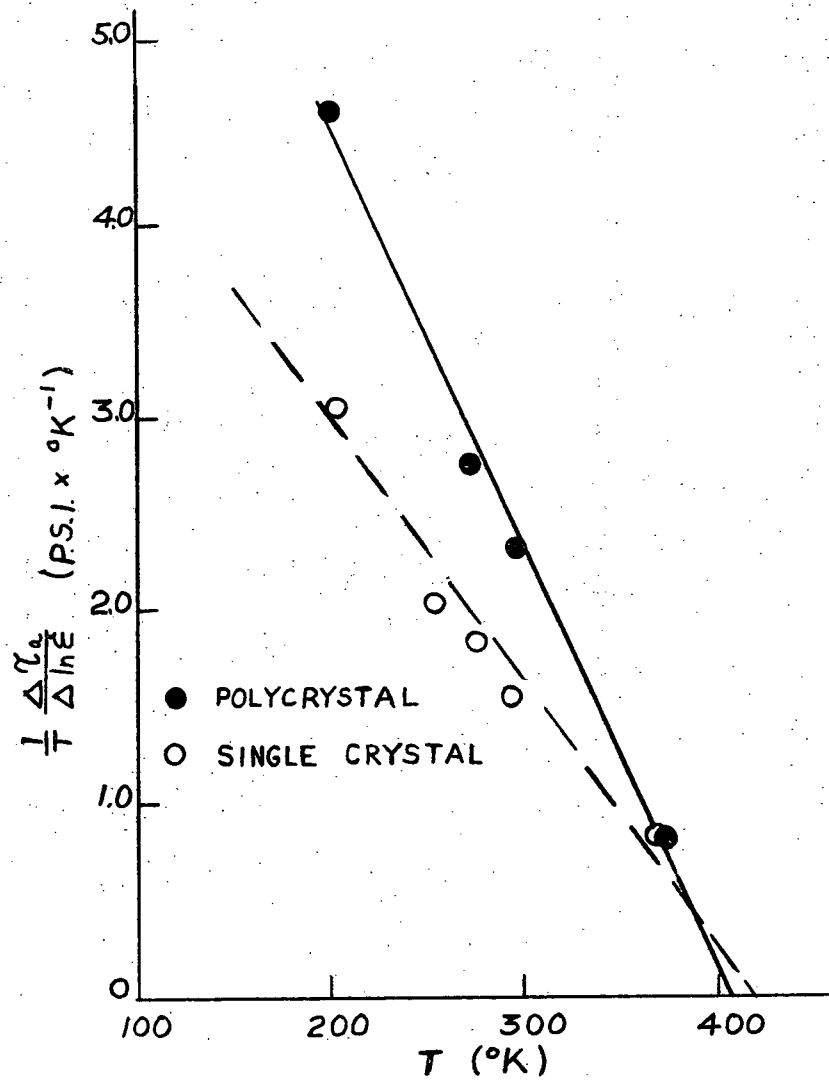


Figure 24a. Strain rate sensitivity of  $\Delta \tau_a$  vs. temperature.

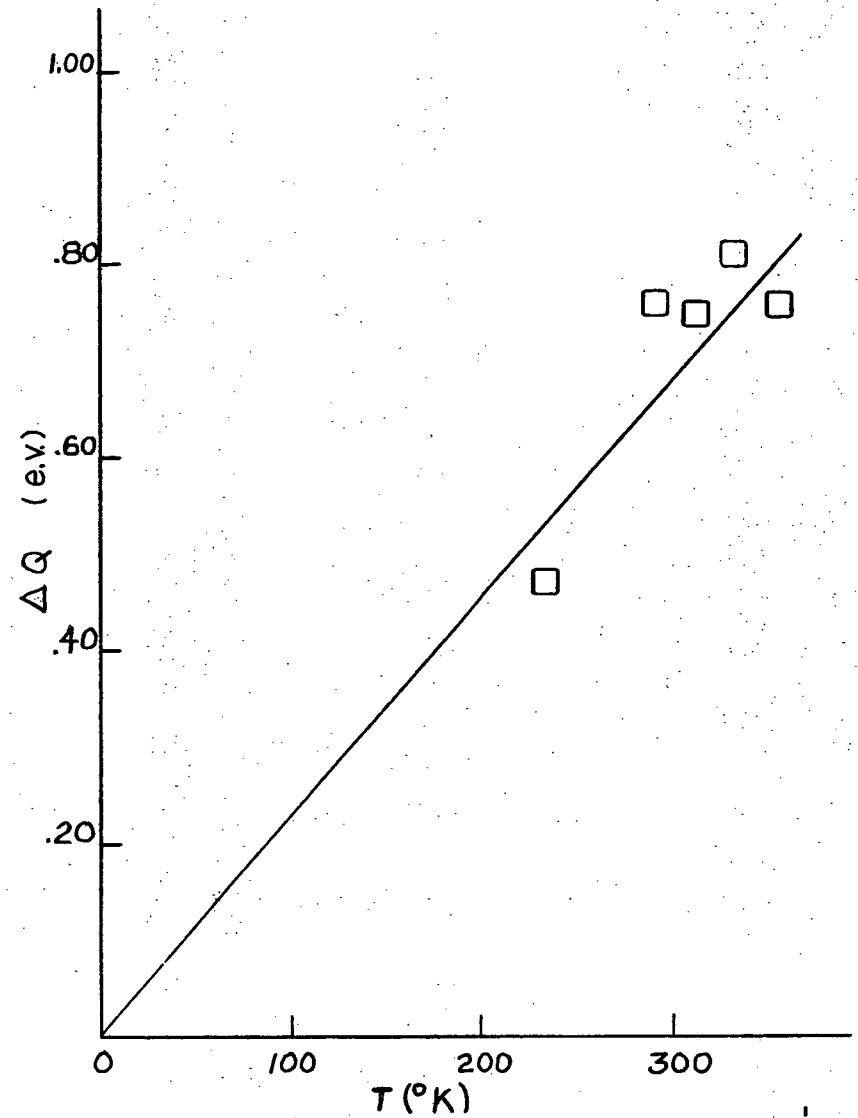


Figure 24b.  $\Delta Q$  vs. temperature for single crystals.

the deformation process will be completely thermally activated and  $\Delta Q = H^{\circ}$ . Thus if Figure (24) is extrapolated to the temperature,  $T_c$ , at which

$$\frac{1}{T} \frac{\Delta \tau_a}{\Delta \ln \dot{\epsilon}} = 0, \text{ then } H^{\circ} \text{ can be calculated from equation (9).}$$

$$H^{\circ} = kT_c \ln(A/\dot{\epsilon}) \quad (18)$$

Taking a value for  $\ln(A/\dot{\epsilon})$  of 25 from Figure (23) and a value for  $T_c$  of  $410^{\circ}\text{K}$  from Figure (24),  $H^{\circ}$  is found to be approximately 0.9 e.v.

Since  $H = 2.3$  e.v. at 10% strain, this suggests that about 1.4 e.v. goes into overcoming the internal stress  $\tau_1$ .

## B. Single Crystals

### 1. Zone Refining

Laué back reflection photographs were taken of each single crystal specimen after machining and electropolishing to determine the orientation and to ensure that any surface deformation caused by machining was removed. Figures (25a) and (25b) show Laué spots for a sufficiently polished and an insufficiently polished specimen. It was necessary to remove about .005" to obtain sharply defined spots.

The orientation of each specimen was plotted and all specimens were found to be of the same orientation to within  $2^{\circ}$ . The position of the tensile axis with respect to the standard stereographic triangle is shown in Figure (26).

Figure 25b. Laué photograph of an insufficiently polished specimen.

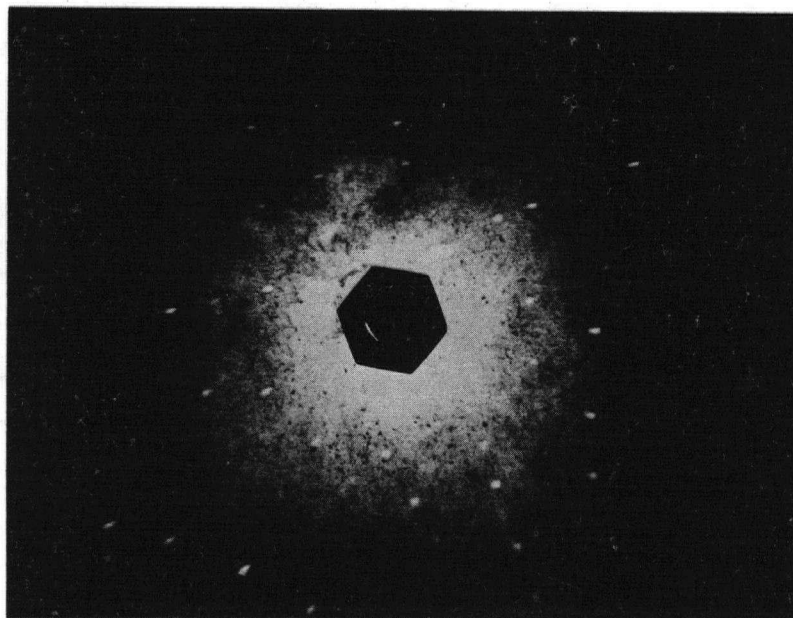


Figure 25a. Laué photograph of a sufficiently polished specimen.

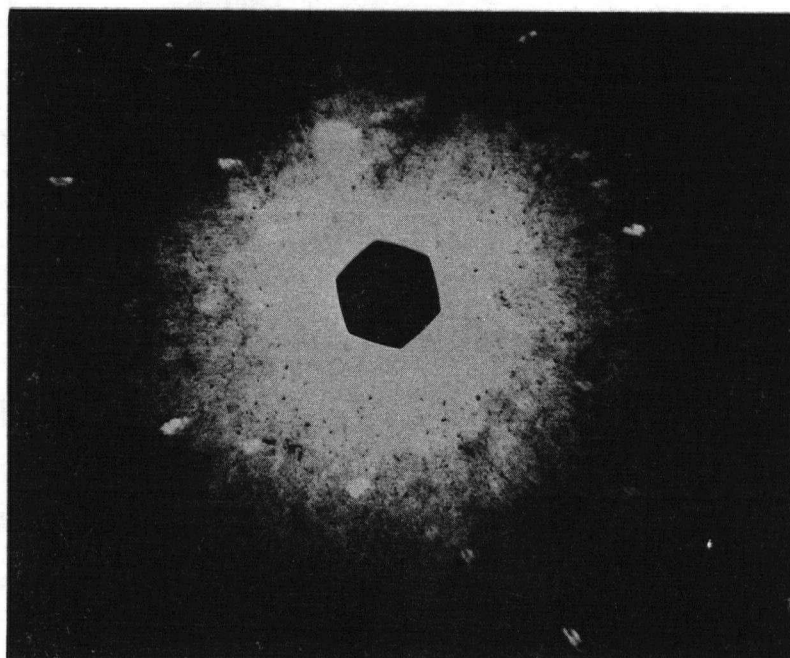


Figure 25b. Laué photograph of an insufficiently polished specimen.

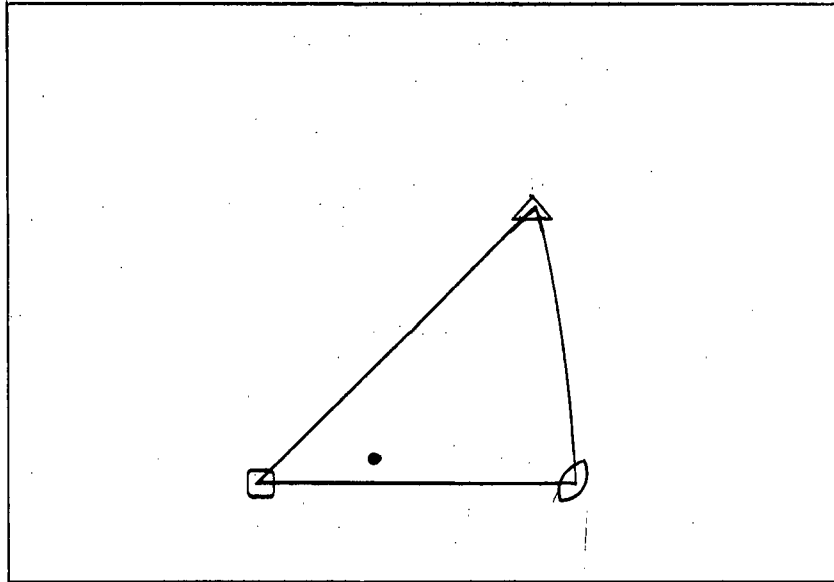


Figure 26. Orientation of tensile axis of single crystals.

The single crystal rods were all radiographed and found to contain a number of small gas holes. These were also observed while the specimens were being polished during which the holes would appear as small surface pits. A photograph of a pitted specimen is shown in Figure (27).

## 2. Slip Systems

Metallographic examination of the deformed single crystals revealed that at least two slip systems were operative during deformation. Near the necked region evidence of three or more systems was frequently observed. Typical slip traces are shown in Figure (28).

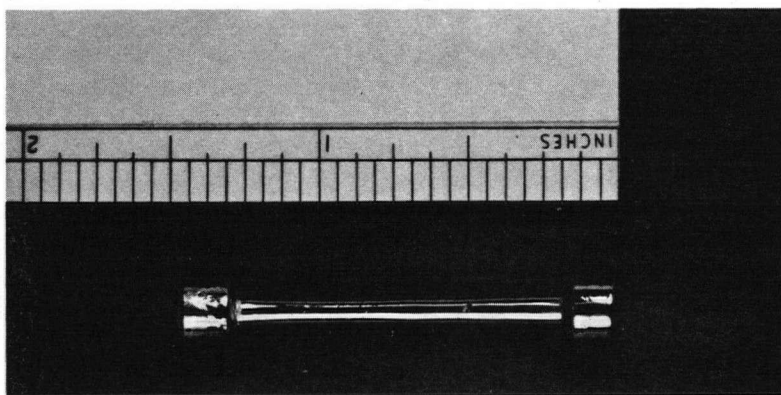


Figure 27. Gas holes in single crystal specimens.

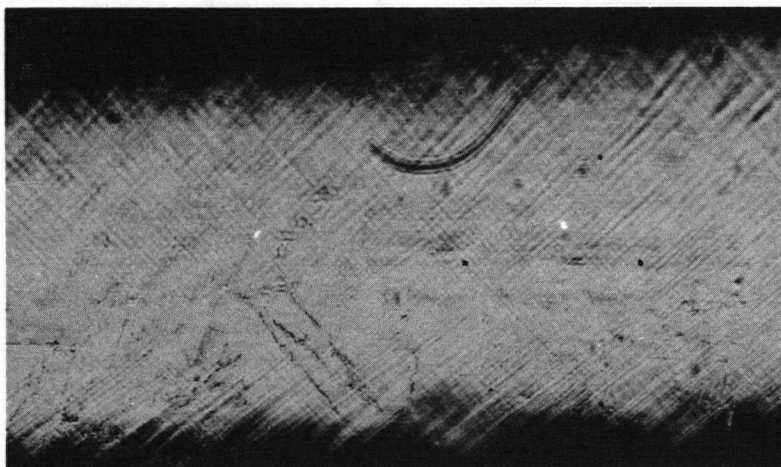


Figure 28. Typical slip traces on single crystal, specimen 6A, 210X.

The slip direction was found to be  $\langle 111 \rangle$ . Due to the complexity of separating the slip markings of the systems involved, an attempt to determine the slip planes was abandoned.

It is already known that the slip planes in a b. c. c. metal are  $\{110\}$ ,  $\{112\}$  and  $\{123\}$ . Using the known orientation and a stereographic projection, the angles between the tensile axis and all of the possible slip planes were measured. From these angles Schmid factors were calculated and the largest of these are tabulated in Table III.

TABLE III  
Possible Slip Systems

Slip Direction	Slip Plane	Schmid Factor
[111]	(10 $\bar{1}$ )	.468
[ $\bar{1}$ 11]	(101)	.482
[111]	(11 $\bar{2}$ )	.468
[ $\bar{1}$ 11]	(1 $\bar{1}$ 2)	.456
[111]	(21 $\bar{3}$ )	.483
[ $\bar{1}$ 11]	(2 $\bar{1}$ 3)	.500

The Schmid factors are roughly the same for each type of slip plane. Because of this, an average factor of 0.48 was used to calculate the resolved shear stress in the single crystals.

### 3. Strain Rate Change Tests

These tests were carried out using the same strain rates as for the polycrystals. The results are plotted in Figures (29) and (30).

$\Delta \tau_a$  is essentially independent of strain and stress at 0°C and 100°C. At -72°C  $\Delta \tau_a$  appears to decrease with deformation. The increase of  $\Delta \tau_a$  with  $\tau_a$  and  $\epsilon$  shown by specimen 5A is too small to be regarded as definite.

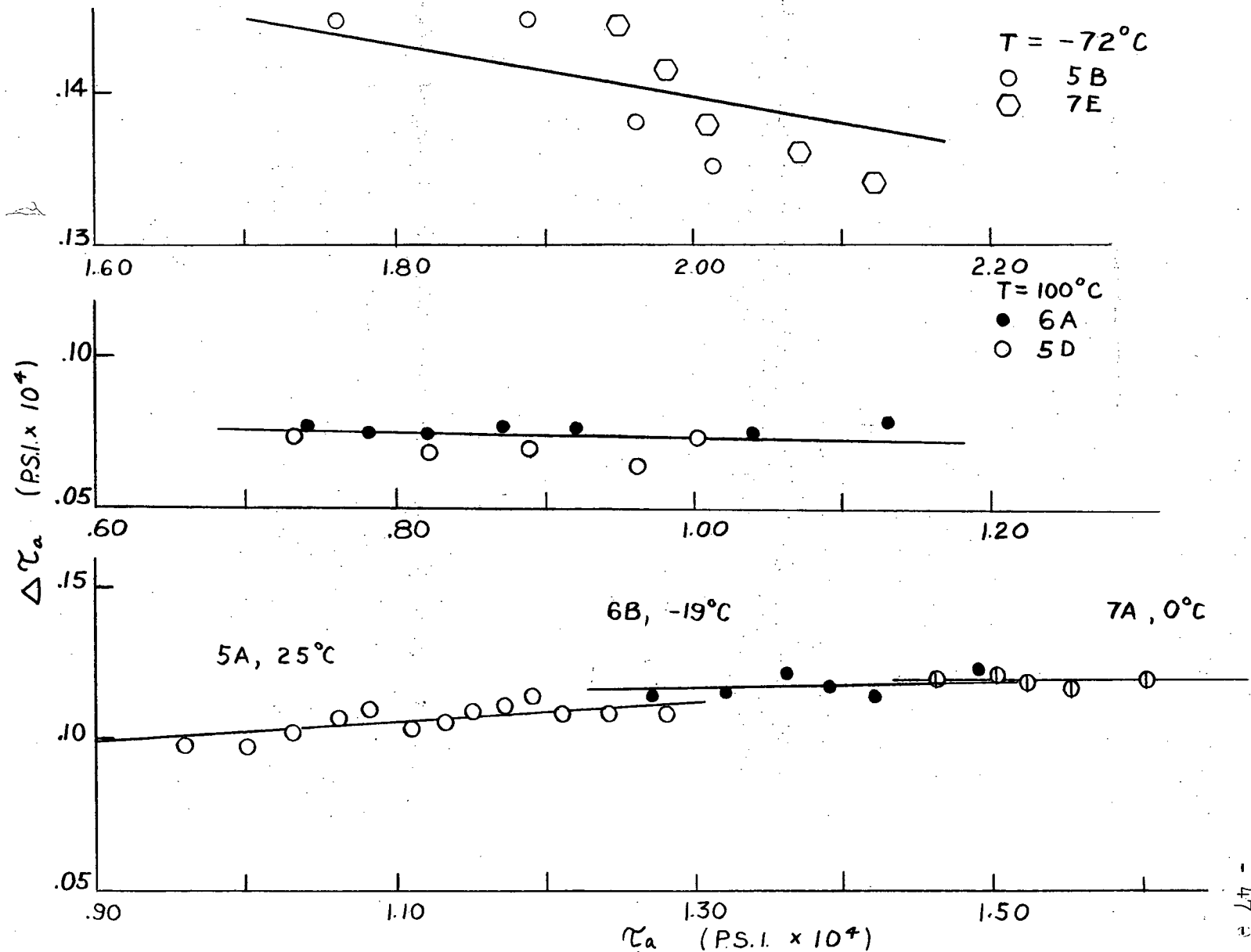


Figure 29.  $\Delta\tau_a$  for an increase in  $\epsilon$  vs.  $\tau_a$  for single crystals.

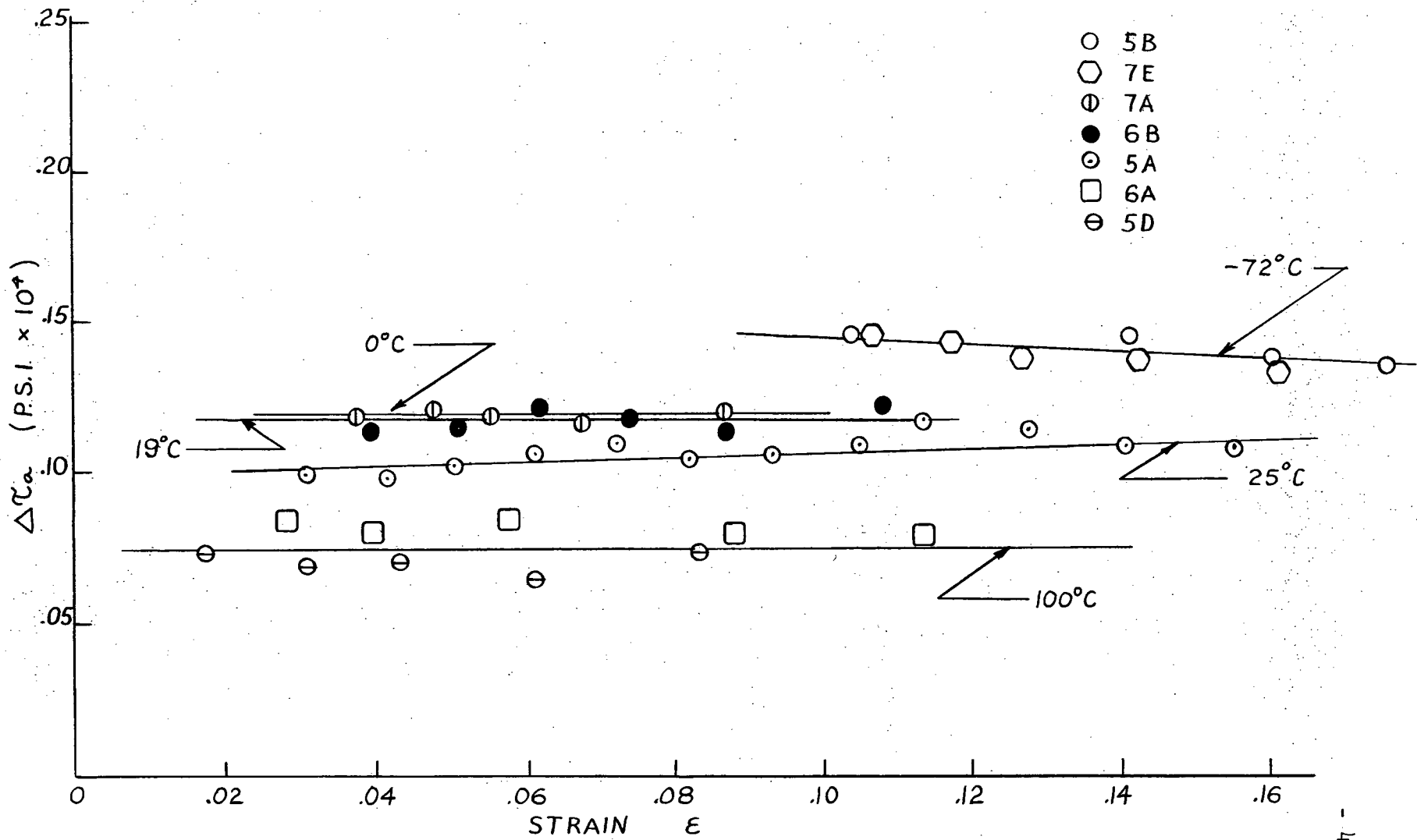


Figure 30.  $\Delta \tau_a$  for an increase in  $\dot{\epsilon}$  vs.  $\epsilon$  for single crystals.

It is evident that the results for single crystals are not as reproducible as those for polycrystals. The reason for this may be the gas holes in the single crystal specimens.

Due to the limited ductility of vanadium below 200° K most of the tests were performed above this temperature. However, one crystal was tested at 78°K to determine the strain rate sensitivity of the flow stress at this temperature. It was possible to cycle the strain rate only twice before the specimen failed so determination of the dependence of  $\Delta \tau_a$  on  $\dot{\gamma}_a$  and  $\epsilon$  was not possible.

The specimen showed evidence of twinning at this temperature. Sudden reductions of stress occurred in the elastic region accompanied by a sharp cracking sound. Metallographic examination revealed twin like markings on the surface of the specimen (Figure (31)). Also a Laué back reflection photograph of the supposed twinned region was taken using a beam in the form of a long narrow slit (Figure 32). Each spot on the film is slit in an identical manner. Small spots corresponding to the gaps were not definitely observed but they could have been masked by the background radiation. The two slits seen in the photograph correspond to two bands of narrow twins with a spacing of about 2 mm. between them.

It should be noted that Snowball<sup>17</sup> in his work on vanadium, did not observe twinning down to 78°K. However, his specimens were of a different orientation, which could explain this disagreement.



Figure 31. Twin markings on surface of a single crystal.

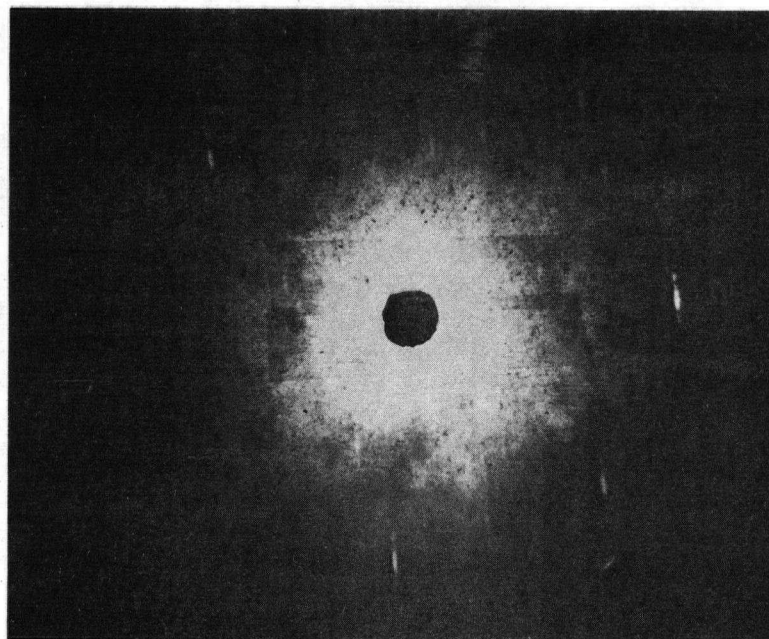


Figure 32. Laue photograph showing slits in spots due to twins.

#### 4. Temperature Change Tests

The temperature change tests were done mainly between  $100^{\circ}\text{C}$  and some lower temperature although one test was performed between  $0^{\circ}\text{C}$  and  $-72^{\circ}\text{C}$ . The results of these tests are plotted in Figures (33) and (34). In all cases, except for specimen 6D,  $\Delta \tau_a$  decreases slightly with deformation. Since only four points could be obtained for 6D, it cannot be definitely concluded that  $\Delta \tau_a$  increases with  $\tau_a$  for this specimen.

#### 5. Rate Equation

The activation volume for each specimen which was subjected to a strain rate change test was calculated and plotted as a function of stress and temperature in Figures (19) and (20). As for the polycrystals, an average value for  $v^*$  was used in the plot of  $v^*$  against temperature.

The activation volume is generally larger for the single crystals than for the polycrystals at any given temperature. This difference decreases as the temperature increases to  $100^{\circ}\text{C}$  where  $v^*$  is the same for both types of specimen.

The energy,  $H$ , was calculated from equation (14) and is plotted as a function of strain in Figure (21).

$\Delta Q$  at 10% strain was calculated from equation (15) for the various mean testing temperatures and is plotted as a function of temperature in Figure (24b) assuming  $\Delta Q = 0$  at  $0^{\circ}\text{K}$ .

$\Delta Q$  was also calculated from equation (8) and is plotted as a function of strain in Figure (22).  $\Delta Q$  again shows a small tendency to decrease with strain although this decrease is not as marked as for the polycrystals.

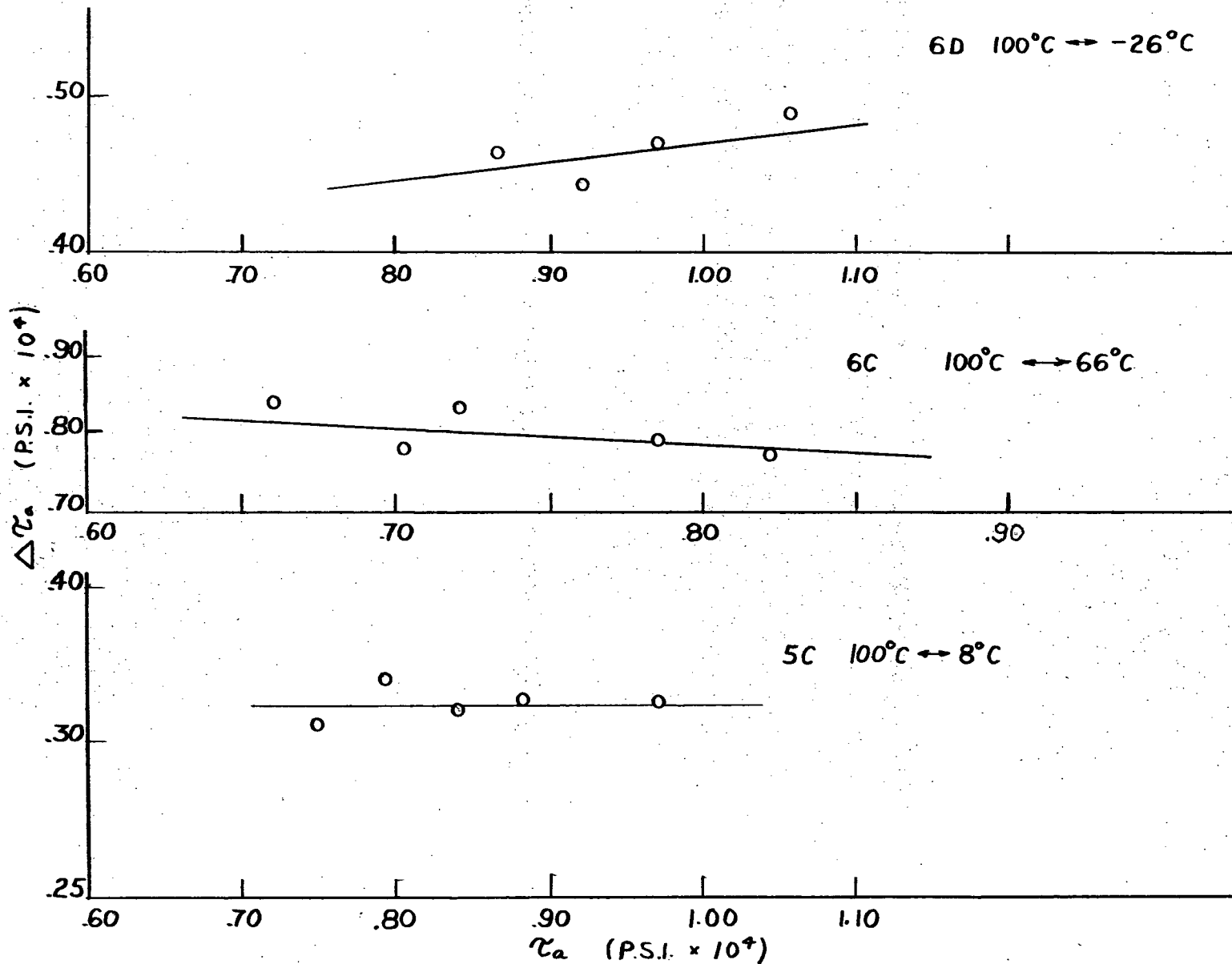


Figure 33.  $\Delta\tau_a$  for a decrease in temperature vs  $\tau_a$  for single crystals.

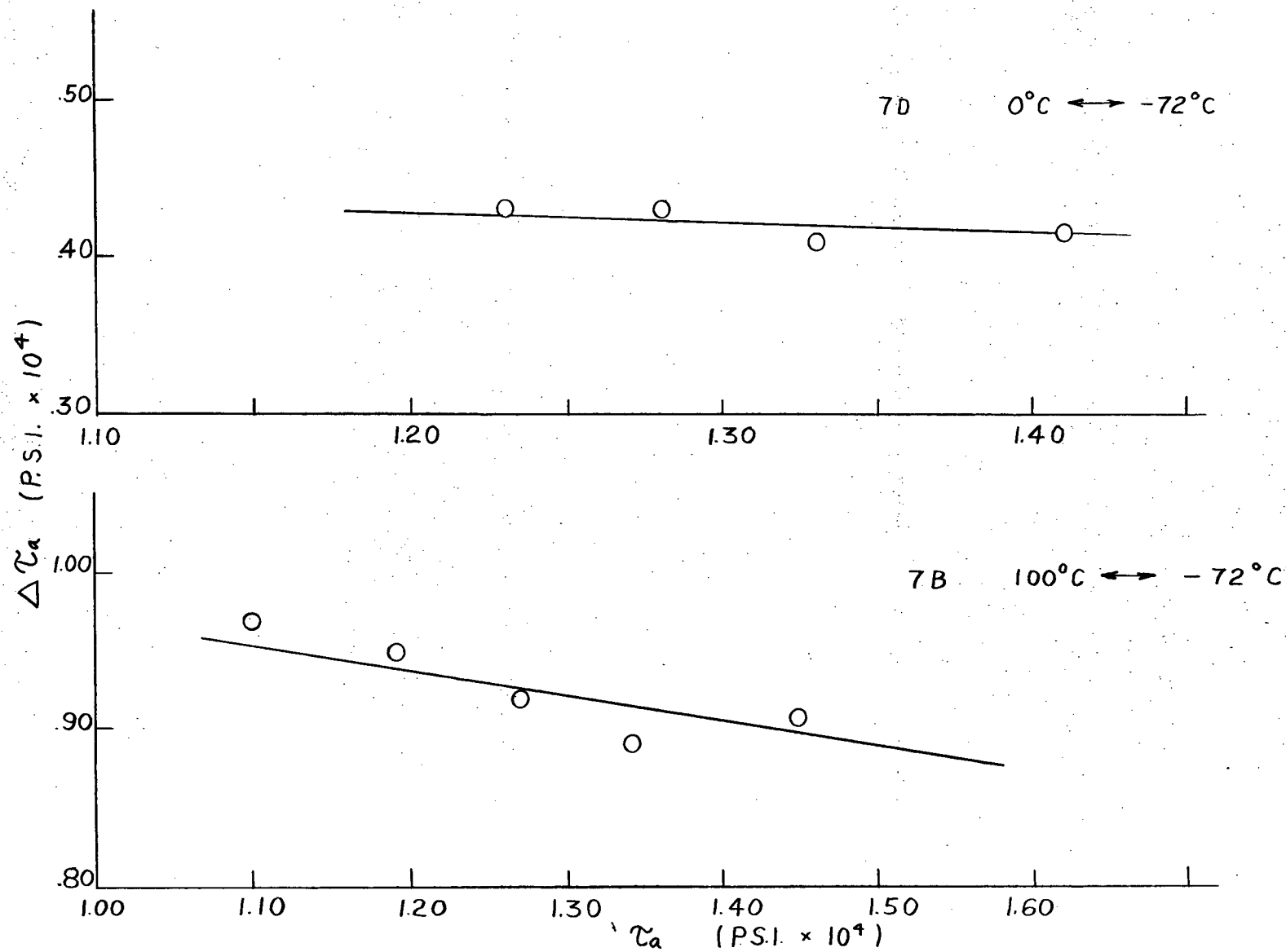


Figure 34.  $\Delta \tau_a$  for a decrease in temperature vs.  $\tau_a$  for single crystals.

An average value for A at 10% strain was calculated by plotting

$\frac{\Delta \tau_a}{\Delta T}$  against  $\frac{1}{T} \frac{\Delta \tau_a}{\Delta \ln \dot{\epsilon}}$  in Figure (35). This yielded a value for

$\ln(A/\dot{\epsilon})$  of 25.9 which is quite comparable to that for the polycrystalline material.

## 6. Yield Points

Yield points similar to those observed during the tests on polycrystals also appeared in the single crystal tests. They appeared under the same temperature conditions as for the polycrystals but in this case they did not show up until after about 5% strain. They increased in size somewhat with increasing strain but they were always smaller than those observed during the polycrystal tests.

One test was performed by straining continuously to 20% strain at the basic strain rate and then the rate was increased by a factor of ten. This was done to determine whether the size of the yield drop depended on the amount of loading and unloading of the specimen. A sizeable yield point was obtained which compared quite favourably with those at the same amount of strain in a normal test. This is shown in Figure (17).

A summary of the results is included in Table IV.

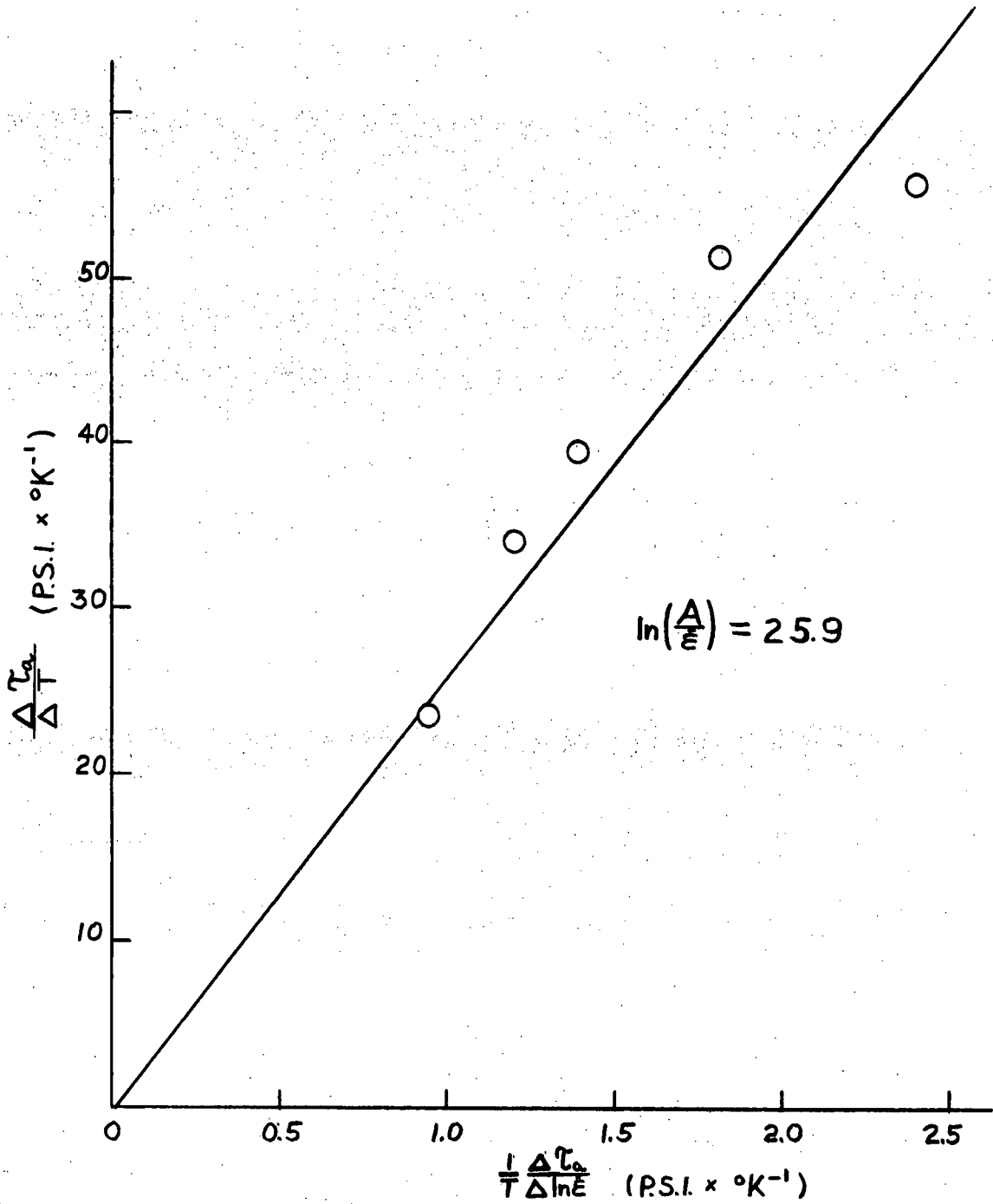


Figure 35. Strain rate sensitivity of the flow stress vs. temperature sensitivity to find  $\ln(A/\dot{\epsilon})$ . (equation (15)).

C. Summary of Results

1. The lower yield stress and the flow stress of vanadium both obey Hall-Petch equations.
2. The slopes of the yield stress and flow stress versus  $d^{-1/2}$  plots are not identical for vanadium.
3. The slope,  $k_{LY}$ , increases with temperature.
4. Vanadium does not obey the Cottrell-Stokes Law.  $\Delta \tau_a$  is constant or decreases slightly with  $\tau_a$ .
5.  $\Delta \tau_a$  is independent of grain size over the range tested.
6. The activation volume for single crystal specimens diverges from that for polycrystals at low temperatures.
7. The activation energy,  $H^\circ$ , is roughly 1 e. v. for thermally activated flow in vanadium.
8. Yield points are observed upon reloading a specimen in tests involving a temperature of  $100^\circ\text{C}$ .
9. Vanadium deforms by twinning at  $-196^\circ\text{C}$  when the orientation is as in Figure (26).

TABLE IV

Summary of Results

Specimen	T	H(ev), $\epsilon = 0.1$	Q(ev), $\epsilon = 0.1$	$H^Q$ (e.v.)	$\ln(A/\dot{\epsilon}), \epsilon = 0.1$
Single Crystals	287	1.7	.76	0.9	25.9
	327	1.5	.81		
	310	1.5	.75		
	356	1.4	.76		
	237	1.3	.47		
Poly- Crystals	327	2.3	.72	0.9	25.2

#### IV. DISCUSSION

##### A. Hall-Petch Equation

From the preceding results come two interesting observations:

1.  $k_{LY}$  increases with temperature.
2.  $k_{LY}$  is not equal to  $k_{f1}$ .

Let us first look at the temperature dependence of  $k_{LY}$ . On the basis of Cottrell's theory,  $k_{LY}$  should depend on the stress to unlock dislocation sources pinned by impurity atoms. Hence, one expects that  $k_{LY}$  should decrease with increasing temperature. However, just the opposite is observed. This suggests that the Cottrell theory is an over-simplification.

These observations differ from those of other workers<sup>5,6</sup> in that their  $k_{LY}$  values were independent of temperature. Conrad<sup>5</sup> points out that a temperature independent  $k$  could be explained in terms of an athermal unlocking process.

If one attempts to use this idea to explain a  $k$  which increases with temperature one must have an  $l$  (the distance from the pile up to the nearest source in the next grain) which increases with temperature. Such a situation is difficult to understand.

Conrad's suggestion that the differing heat treatments given to the specimens may be responsible for the behavior of  $k_{LY}$ , is worthy of discussion. If the sources are pinned dislocations, then those specimens annealed at a higher temperature (larger grains) might be expected to have fewer sources. This would result in a larger value for  $l$  (equation (6))

than in fine grained specimens. However, for any given grain size  $l$  should be the same and while differing heat treatments may affect the actual values for  $k_{LY}$ , it is hard to see how it could affect the relative values over a range of temperature.

The difference between  $k_{LY}$  and  $k_{f1}$  is not surprising. Conrad assumes that because  $k_{f1} = k_{LY}$  in his measurements the same deformation mechanism is involved in yielding as in flow. His  $k_{f1}$  was measured at a strain of .05 as it was in this work.

In a polycrystalline specimen considerable work hardening occurs near the grain boundaries. Hence, one might expect that the flow stress at five percent strain would depend on the grain size through the rate of work hardening in the grains and this is not necessarily related to the lower yield stress. An equivalence between yielding and flow mechanisms would then suggest an equivalence between the activation and stopping of sources and there is no sound reason to make this assumption.

The results of this work are in disagreement with the work of Conrad and it appears as if his conclusions were premature. No alternative explanation of these processes can be given here because of the limited scope of this portion of the research. A large scale research programme is required involving several different b. c. c. metals.

#### B. Thermally Activated Flow

At present there exist the following suggested mechanisms for controlling the thermally activated flow of dislocations in body-centered cubic metals:

1. Intersection with a forest
2. Impurity atoms interacting with dislocations
3. Cross slipping of screw dislocations
4. Large Peierls stress
5. Non-conservative motion of jogs in screw dislocations

1. Intersection with a Forest

The forest mechanism, although quite acceptable for f. c. c. metals, is probably the least acceptable for b. c. c. metals.

At the beginning of deformation it is unlikely that the forest density would be greater than  $10^8$  dislocations per square centimeter. If a uniform distribution of forest dislocations is assumed this would lead to a spacing of  $10^{-4}$  cm. between the "trees" of the forest. A typical value for the activation volume of vanadium is  $10^{-21}$  cm<sup>3</sup>. Now assume that  $d$ , the activation distance, is of the same order of magnitude as  $b$ , the Burger's vector. This is not unreasonable as any thermally activated process must involve short range forces. The distance between obstacles is found to be  $L = \frac{v^*}{b^2} \approx 1.5 \times 10^{-6}$  cm. This is a smaller spacing than one would expect for a uniformly distributed forest.

It has been observed<sup>21</sup> that in f. c. c. metals the dislocations are distributed non-uniformly, that is, they exist as tangles alternating with relatively dislocation free areas. It is pointed out that the flow stress is determined by the spacings in these tangles. These tangles could have a smaller spacing between the "trees" of the forest and therefore be consistent with the measurements in this research. However, this

type of dislocation structure is not generally observed in b. c. c. metals, in fact, Gregory's electron micrographs show a relatively uniform distribution. Also, it has been pointed out by Wilsdorf<sup>22</sup> that the spreading of these tangled regions into dislocation free regions corresponds to stage I or easy glide in f. c. c. metals, and at the beginning of stage II the distribution is relatively uniform. All of the measurements in this work were taken in the later stages of deformation after heterogeneous yielding had ceased.

The activation energy for a forest mechanism will depend on the short range forces on the moving dislocations. Since dislocations in b. c. c. metals are generally non-extended these forces would be related to the energy of jogs formed during intersection. This energy is generally estimated to be  $\mu b^3/10$  which, assuming a shear modulus of  $4.6 \times 10^{11}$  dynes/cm<sup>2</sup> yields an activation energy of roughly 0.5 e.v. This is somewhat smaller than the measured values in this work but it does not disagree enough to discount the forest mechanism on this basis alone.

Because of the numerous active slip systems in b. c. c. metals one would expect the forest density to increase greatly with deformation, say at least by a factor of one hundred over the complete range of strain. In a uniform forest this would lead to a tenfold decrease in the activation volume with strain and a tenfold increase in  $\Delta \tau_a$ . The results of this research do not show this trend.

If the forest is non-uniform and spreads by the expansion of tangled regions into clear ones, then the activation volume could remain constant if flow is controlled by the spacing in the tangles. However, if

this structure did exist the tangled regions would soon cover the whole specimen and one might expect to see a change in  $v^*$  in the latter stages of deformation. This is not observed.

It would seem likely by these arguments that the forest mechanism does not control thermally activated flow in vanadium.

## 2. Impurity Atoms

The interaction of a uniform distribution of interstitial impurities with moving dislocations has been proposed as a possible mechanism responsible for the thermal component of the flow stress.

The work of Heslop and Petch<sup>4</sup> on iron suggests that the temperature dependent part of  $\sigma_{f1}$  does not depend on the amount of C + N in solution.

Calculations<sup>23</sup> using linear elasticity theory indicate that the interaction energy between an interstitial carbon atom and a dislocation in iron is about 1 e.v. However, it is pointed out that the use of linear elasticity theory almost certainly would yield an over-estimation. This energy is calculated from equation (19).

$$E = \frac{\mu b}{3\pi} \frac{1+\nu}{1-\nu} \frac{\sin\theta}{r} \Delta V \quad (19)$$

Where E is a maximum for  $\theta = \frac{3\pi}{2}$  and  $r = b$ , and  $\Delta V$  is the volume change due to one interstitial per unit cell. The shear modulus,  $\mu$ , for vanadium is slightly more than one half of that for iron. Also, since the lattice parameter is larger for vanadium than for iron it is likely that  $\Delta V$  will also be smaller. Hence, a maximum value for E in vanadium would be roughly 0.5 e.v.

We would expect the activation volume for an interstitial mechanism to decrease slightly with strain. The number of interstitials will not change with strain and therefore the activation length,  $L$ , will not change. The activation distance,  $d$ , should decrease somewhat since as the flow stress increases with work hardening the dislocation will rise to a higher level on the force-distance curve. The observed activation volume is relatively constant with strain or in some cases increases slightly in disagreement with an interstitial mechanism.

If the interstitials are assumed to be uniformly distributed one can calculate the spacing  $L$  in the activation volume. In the polycrystalline material there is roughly one interstitial per 1000 atoms. This is equivalent to an interstitial in every 500 unit cells and an average spacing of  $\sqrt[3]{500} a \approx 8 a$  where  $a$  is the lattice parameter. Thus we have a spacing between the interstitials of roughly  $2.5 \times 10^{-7}$  cm. This is too small to agree with the measured value for  $L$  in this work. For the single crystals  $L$  would be  $3 \times 10^{-7}$  cm. which is also too small to agree with this work.

It might be argued that the interstitials may be segregated due to the presence of dislocations and tend to be closer together along dislocation lines before straining. However, it is likely that saturation of dislocations would occur before a large fraction of the interstitials could segregate and therefore the average spacing should not be too far from that for a uniform distribution.

### 3. Cross Slipping of Screw Dislocations

Observation of wavy slip lines in b. c. c. metals has been interpreted as evidence of cross slipping of screw dislocations. This process has been described by many authors<sup>24</sup>. It involves a screw segment of an obstructed dislocation loop cross slipping to a parallel slip plane. The screw segment is locked in the new slip plane by an edge dipole which is formed in the cross slip process. Multiplication occurs when the locked screw segment acts as a Frank-Read source.

Johnston and Gilman<sup>25</sup> have shown that the ease with which such a source operates is inversely proportional to the length of edge dipole or jogs formed in the cross slip process. The stress to operate a source is given by

$$\tau_a = \frac{\mu b}{8\pi(1-\nu)} \frac{1}{d^1} \quad (20)$$

Where  $d^1$  is the spacing between the new and old slip planes. Assuming  $\nu = 0.3$  (Poisson's ratio) and taking  $\tau_a = 4 \times 10^4$  psi. which is as high an applied stress as any specimen received one finds  $d^1 = 30 \times 10^{-8}$  cm. or  $d^1 = 11b$ .

This is a minimum value for  $d^1$  since in most tests the applied stress was less than  $4 \times 10^4$  psi. This distance is too great to be effectively overcome by thermal fluctuations and the energy of the edge dipoles produced in the process would be prohibitive.

### 4. Peierls-Nabarro Force

The idea of the Peierls-Nabarro force as the mechanism controlling thermally activated flow is a popular one. However, the choice of this

mechanism has in most cases been somewhat arbitrary. Heslop and Petch<sup>4</sup> chose it for lack of a better one rather than as a result of any intensive study. Actually a high Peierls stress might be expected for b. c. c. metals since departure from close packing should favour the narrowing of dislocations.

It is difficult to support this mechanism on the basis of numerical results. The Peierls force will be large only for dislocations lying in close packed directions, that is,  $\langle 111 \rangle$  in b. c. c. There is no reason for assuming that most of the dislocations are of this type although electron microscopy studies on silicon iron<sup>26</sup> do support this, (Figure (36)).

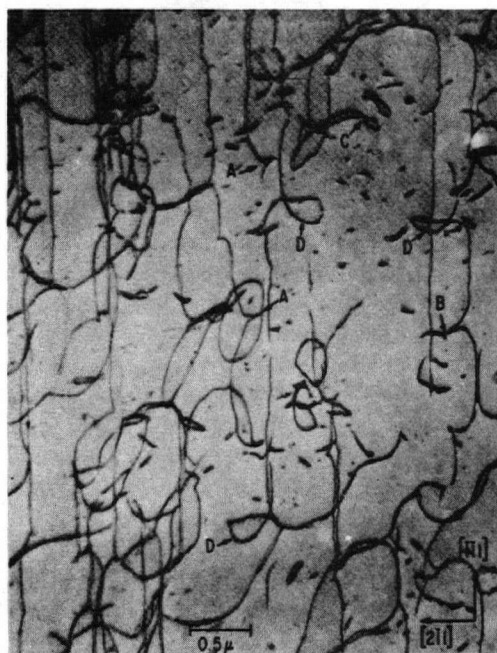


Figure 36. Transmission electron micrograph of dislocations in silicon iron, after Low and Turkalow.

However, this is a particular case. One must keep in mind the work of Stein and Low<sup>27</sup> who showed that the mobility of edge dislocations is approximately twenty times that for screw dislocations in silicon iron. Since the slip direction is  $\langle 111 \rangle$  one would expect to observe loops with extended screw segments. The deformation takes place mainly by edge dislocations which are not oriented to experience a large Peierls force. This behavior has not been observed in any pure b. c. c. metal.

The Peierls mechanism is based on a series of energy maxima and minima parallel to the dislocation line as in Figure (37).

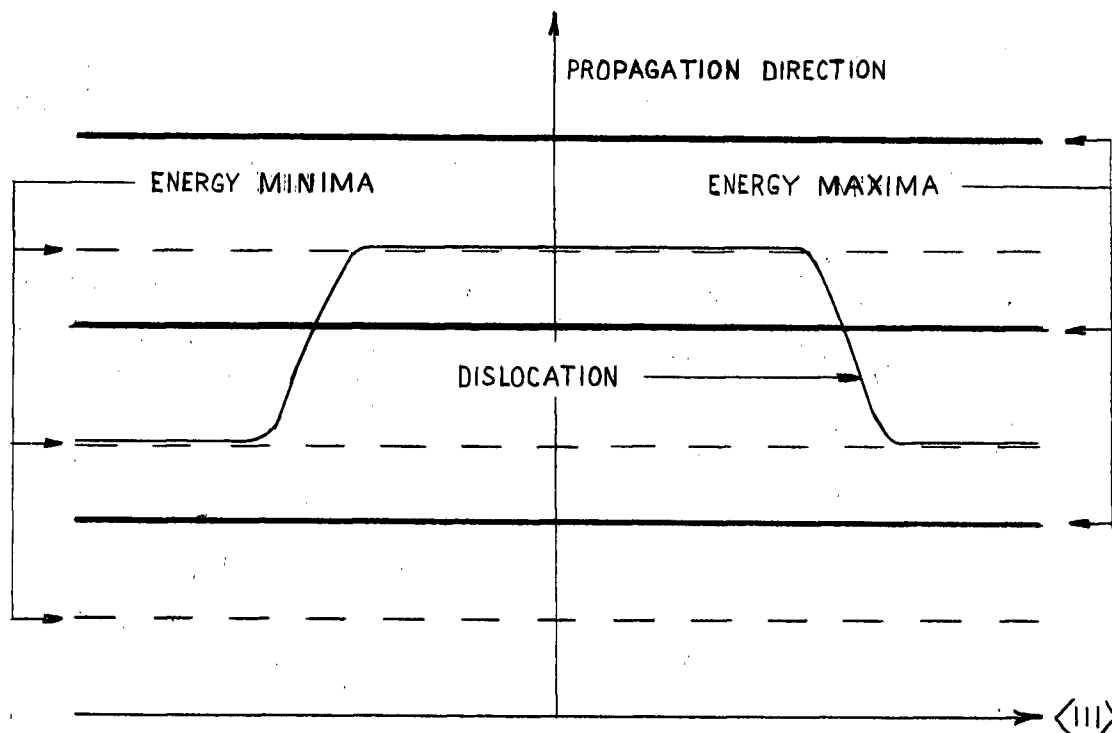


Figure 37. Formation of a dislocation kink in a Peierls force field.

The Peierls mechanism would operate in the following manner. In order that a dislocation propagates, a segment of a critical length,  $L_{cr}$ , must overcome the barrier.  $L_{cr}$  is determined by the attractive force between two kinks of opposite sign and the applied stress. If the loop segment is longer than  $L_{cr}$  then the kinks will propagate in opposite directions and the dislocations will move forward. Thus  $L_{cr}$  is determined by the applied stress  $\tau_a$ . At lower temperatures  $\tau_a$  is larger and therefore  $L_{cr}$  can be smaller than at high temperatures. This would be helpful in explaining the dependence of  $v^*$  on temperature.

Read<sup>28</sup> has pointed out that the controlling factor in this process is the formation of a kink. The sideways motion of a kink occurs with relative ease compared with the forward motion of the dislocation against the high Peierls stress.

Seeger<sup>29</sup> has calculated the kink energy in a publication on an internal friction peak due to kink formation in copper. Because of the many "a priori" assumptions in this calculation a reliable estimate for vanadium cannot be made. To obtain a value for the kink energy it would be necessary to do internal friction measurements on vanadium. It may be difficult to observe a peak due to kink formation because of the many other internal friction sources in vanadium.

##### 5. Non-Conservative Motion of Jogs in Screw Dislocation

When a screw dislocation acquires a jog, it is of the edge orientation and therefore can glide conservatively only in the direction of its Burgers vector which is parallel to the screw dislocation line.

It will therefore cause a drag on the motion of a screw dislocation. This is also true for jogs in mixed dislocations, that is, any dislocation with a screw component.

If these jogs are to move with the dislocation they must move non-conservatively, leaving behind a trail of vacancies or interstitials. The creation of interstitials is energetically unfavourable. The vacancy mechanism would be governed by the energy of formation of vacancies which is of the order 2 to 3 e.v.

There is some argument against the vacancy mechanism. It has been suggested by Friedel that vacancy jogs might move conservatively along the dislocation loop until they can glide conservatively with the loop or they may combine with jogs of opposite sign and annihilate one another. Frank<sup>34</sup> has pointed out that the former possibility is unlikely as it requires a stationary shape of the dislocation loop. This would require a higher dislocation velocity in regions of convex curvature of the dislocation. It is more likely that the jog will lag behind and either form an edge dipole or move in non-conservative jumps.

The annihilation of jogs would result in an increase in activation volume with strain. Also, even if the jogs do not annihilate each other the spreading of the dislocation loop would result in an increase in the jog spacing. However, new jogs should be introduced continuously by intersection with the forest and it is conceivable that an equilibrium could be set up such that the spacing of jogs remains roughly constant.

It is difficult to believe that such an equilibrium could be set up instantaneously and therefore one might expect to see some evidence of this in the early stages of deformation. In fact, in some of the tests, the largest scatter in the plots of  $\Delta \tau_a$  against  $\tau_a$  was observed for the first point.

The main objection to the vacancy mechanism here is that the measured activation energy is small. The energy of formation of vacancies in b. c. c. metals is roughly 2 to 3 e. v. which is not very compatible with the measured value of  $H^0 \approx 1$  e. v. for vanadium. There is some question, however, as to the validity of assuming the energy to form a vacancy at a jog is the same as that for forming one in a perfect lattice. It is known for instance that the energy to form a vacancy in an alloy is much less than that for the pure metal. Unfortunately a detailed analysis of this problem would require sophisticated quantum mechanical calculations which are beyond the scope of this work.

#### 6. Comparison Between Polycrystals and Single Crystals

The divergence between polycrystals and single crystals in the plots of  $v^*$  against temperature is difficult to explain. On the basis of an interstitial mechanism, the polycrystal curve should lie below that for the single crystals since the polycrystals have a higher interstitial content. This would result in a smaller activation length,  $L$ , and hence a smaller activation volume. However this would not explain the convergence of the two curves with increasing temperature.

It is possible that the difference in  $v^*$  lies in the activation distance,  $d$ . This might be brought about by a difference in the shapes

of the force-distance curves for the two materials. It is difficult to explain why this should occur if the same mechanism is operative in both types of specimens.

On the basis of a vacancy jog mechanism the energy to form a vacancy may depend on the internal stress field. From the measurements of  $H^0$  and  $H$  it appears that the internal stress field is larger for the polycrystalline specimens. This could be responsible for a difference in the shapes of the force-distance curves.

The value of the factor  $A$  in equation (9) is roughly the same for the two materials. The trend for  $A$  to decrease by  $10^2$  to  $10^3$  with strain might be explained by a decrease in the number of mobile dislocations. One would not expect  $\lambda$  or  $\nu$  to decrease by more than a factor of five with strain. A decrease in the number of mobile dislocations means those remaining must move at a higher velocity which would result in an observed work hardening.

## 7. Mechanism

It is rather difficult to pick out a single mechanism as the controlling one in thermally activated flow. The fact that the opinions of so many authors differ is evidence enough for that. What is generally done is to select a mechanism which fits the data best and declare this to be the most probable one.

On the basis of the preceding arguments it is reasonably safe to rule out the forest, cross slip and interstitial mechanisms on the

grounds of severe disagreement between theory and experiment. The Peierls mechanism can not be compared with the data because it is not possible to calculate  $v^*$ ,  $H^0$  and  $A$  accurately from theory. Certainly the important point here is whether the dislocations do lie predominantly in the  $\langle 111 \rangle$  directions. There is not sufficient evidence available at this time to answer this question.

The jog mechanism is the best one for explaining the increase in activation volume with strain which was observed in some specimens. The jogs are the only obstacles which could spread apart with deformation. An argument against the jog mechanism is that it cannot operate at low temperatures. This is because the vacancy formed must diffuse away immediately or it will draw the jog back again. At low temperatures this diffusion might be difficult.

On the basis of preceding arguments it appears as if the Peierls mechanism is the most likely one. However, this may be just because there is insufficient evidence available to dispute it.

What one should inquire at this juncture is just how valid is the application of rate theory to this process. It has been assumed that there is a single thermally activated mechanism operative. In fact, it is possible that the average effects of two or more mechanisms were measured. Since two mechanisms would likely have different temperature dependences, the predominance of one could change with respect to the other over a range of temperatures.

With the disagreement between theory and experiment in all the proposed mechanisms it is conceivable that more than one mechanism could well be the controlling ones. What is needed at this time is a reliable mathematical analysis of the Peierls mechanism so that its importance in b. c. c. metals can be definitely established.

The assumption used in the derivation of equations 13, 14, and 15, that  $A$  is not significantly dependent on stress, is worthy of discussion. This assumption means that the number of mobile dislocations does not change greatly during a strain rate change. Martinson<sup>30</sup> contends that in LiF the number of mobile dislocations is a sensitive function of the mean stress prevailing during a stress increase. He used this hypothesis to explain his irreversibility of  $\Delta\tau_a$ . He found that  $\Delta\tau_a$  for a strain rate increase was not equal to that for a decrease and also that upon unloading and reloading at the same strain rate the flow stress showed a change.

This type of irreversibility was not observed in this work. The flow stress was completely reversible to within the limits of experimental accuracy.

Also, the strain rate change tests of 100 times yielded a  $\Delta\tau_a$  approximately twice as large as that for a factor of 10 change from the same basic strain rate. If the number of mobile dislocations were to increase with the mean stress prevailing then we would expect  $\Delta\tau_a$  for a change of 100 times to be less than twice that for the factor of 10 change.

### C. Yield Points

The yield points obtained upon reloading after cycling have been observed by many experimenters but have not been satisfactorily explained by any of them. It is important to understand this process however, in order to justify the method of extrapolation used to determine the flow stress in a strain rate or temperature change test.

Some authors have attempted to explain this effect as being a type of relaxation phenomenon. Upon unloading the specimen or even just stopping the crosshead, the dislocations relax into a configuration of lower energy. Hence, energy must be supplied to bring the dislocations from their relaxed configuration back to the pattern which they were in just before the crosshead was stopped. This hypothesis is strengthened by the irreversibility of plastic flow. When a stress is removed from a crystal one might expect the dislocations in pile ups to run back along their slip planes causing large reverse plastic flow. In fact, this does not occur and therefore there must be some obstacles to this process.

Makin<sup>31</sup> has described a process for f. c. c. crystals in which Cottrell-Lomer sessile dislocations are formed on unloading and these prevent large scale reverse plasticity. Since energy is released upon formation of these sessiles a higher stress than the flow stress is required to dissociate them. This would result in an observed yield drop.

Makin observed yield drops at temperatures ranging from  $-195^{\circ}\text{C}$  to  $100^{\circ}\text{C}$ . The magnitude of the drops appeared to be independent of temperature and was proportional to the reduction in stress on unloading. The yield drops in this thesis however were observed only in tests involving

the temperature  $100^{\circ}\text{C}$ , and they showed no dependence on the amount of unloading. These facts, combined with the fact that a mechanism of sessile dislocation formation similar to the Cottrell-Lomer mechanism is not known for b. c. c. metals suggest that Makin's theory does not apply to vanadium.

Birnbaum<sup>32</sup> has also discussed this effect in f. c. c. metals. He suggests that upon unloading, the dislocations relax until they react elastically with forest dislocations and are held. The yield point is a result of releasing the dislocation from its bound configuration. This type of mechanism could certainly be applicable to b. c. c. metals since with the numerous slip planes a high forest density is likely. However, it would be difficult to explain the temperature dependence of the yield drops on this basis. Birnbaum observes that the magnitude of the yield drops are independent of temperature over a range from  $72^{\circ}\text{K}$  to  $293^{\circ}\text{K}$ .

It therefore appears that the yield point effect in vanadium is not controlled by the same mechanism as for f. c. c. metals. The fact that it occurs only at high temperatures or at a low temperature after cooling from  $100^{\circ}\text{C}$  suggests a diffusion controlled mechanism. One might expect that the dislocation becomes locked by interstitials when they stop and an unlocking stress is required to reinitiate flow.

Now the times of relaxation are far too short for the normal diffusion mechanisms. In the strain-rate change tests the crosshead was stopped for less than one minute before reloading while in the temperature change tests the load was relaxed for no more than twenty minutes. In spite of the longer resting periods during temperature change tests the

yield drops showed no significant difference in magnitude from those in the strain-rate change tests.

The interstitial content in the single crystals was about one half of that for the polycrystals and the observed yield drops were smaller for the single crystals. This relationship suggests that interstitials might be involved.

Thus we are looking for a diffusion controlled interstitial locking mechanism which can operate in a very short time relative to normal diffusion times. The only mechanism which seems to satisfy this is Snoek ordering. A brief description of this mechanism will be given.

It is well known that the interstitials in b. c. c. metals cause tetragonal distortion when they occupy the  $(00\frac{1}{2})$  (cube edge) position in the unit cell. There are three types of these sites corresponding to the three directions of tetragonality or the three space axes. Under no applied stress the interstitials should be present in these three sites in equal fractions. However, under an applied stress some sites will be preferable energetically to others and at temperatures where diffusion can take place the interstitials should redistribute themselves so as to increase the population of the sites of lower energy. This is known as the Snoek effect.

Schoeck and ~~Seeger~~<sup>33</sup> state that the stress field of a dislocation should have a similar effect on the interstitials. Hence we expect a redistribution which would lower the energy of the dislocation and therefore lock it. This involves the movement of atoms a distance of only

one atomic jump and could occur in a very short time. This process appears to explain the observed yield drops very adequately.

The actual intent of Schoeck and Seeger was not to explain the yield drops but to explain a temperature independent region on the flow stress versus temperature curve for iron. They show that the Snoek effect will create a friction force on dislocations which is inversely proportional to their velocity.

On the basis of this explanation it would be correct to extrapolate through the yield drop, as was done in this thesis, to obtain the correct value for the flow stress.

## V. CONCLUSIONS

1. A similarity between the mechanisms of yielding and of flow is not observed for vanadium.
2.  $k_{LY}$  increases with temperature for vanadium.
3. Vanadium does not obey the Cottrell-Stokes Law.
4. It is unlikely that the forest, cross slip and interstitial mechanisms control thermally activated flow in vanadium.
5. The controlling mechanism for thermally activated flow is probably either the Peierls-Nabarro force or the non-conservative motion of vacancy jogs. However, there is also some evidence against each of these.
6. It is possible that there is not a unique mechanism controlling thermally activated flow.
7. Vanadium deforms by twinning at 78° K when oriented in certain directions.
8. Yield drops obtained upon reloading are attributed to Snoek ordering.

## VI. RECOMMENDATIONS FOR FURTHER WORK

The results of this research indicate the need for an extensive study into the importance of the Peierls-Nabarro force in b. c. c. metals. This would include internal friction work to determine dislocation kink energies and electron microscopy studies to study the orientation of dislocation lines. Before this is done it is unlikely that any further progress will be made in the work hardening theory.

It would also be interesting to conduct an extensive investigation of the yield point effects. This would involve work at higher temperatures than were used here and a thorough investigation of the dependence of this effect on impurity content.

VII. APPENDICES

APPENDIX I

A. Annealing Data for Grain Growth

Specimen	Annealing Temp. °C	Annealing Time hr.	Grain Size microns
8A	870	1	14.5
8B	940	1	16.6
8C	1020	1	26.5
8D	1090	1	33.4
9A	870	1	17.8
9B	940	1	24
9C	1020	1	35.6
9D	1090	1	52.8
10A *	1090	4	Too large and non-uniform
10B	1050	4	55
10C	995	4	43
10D	900	1.5	Not measured
10E	820	1	12.4
11A,B,C & D	870	1	19.4
11E,F, 12A & B	1020	2	54.6
12C,D,E & F	1090	8	69
13A,B & C	920	1	26.1
13D, E & F	970	2	35

\* Rod 10 deformed 4% before annealing.

APPENDIX II

A. Polycrystals

Specimen	Area of Cross section in. <sup>2</sup>	Gauge length in.	LY P.S.I. x 10 <sup>4</sup>	Testing Temp. °C	Crosshead Speed in.min. <sup>-1</sup>	Approx. Uniform Deformation %	Remarks
8A	.0145	1.045	4.49	25	.02	24	
8B	.0145	1.028	4.69	25	.02	25	
8C	.0137	0.925	4.52	25	.02	25	
8D	.0126	1.015	4.32	25	.02	20	
9A	.0109	1.057	4.48	25	.002-.02	13	
9B	.0102	0.994	4.63	25	.01-0.1	15	
9C	.00800	0.906	Not Observed	100	.01-0.1	12	Loaded non- axially.
9D	.00693	0.962	3.45	100	.01-0.1	13	
10A	.00916	1.048	-	-	-	-	Not tested due to undesirable grain size.
10B	.0141	0.995	3.96	25	.02	18	
10C	.0141	0.942	4.36	25	.02	18	
10D	.0132	0.992	-	-	-	-	Damaged during mounting.
10E	.0137	0.950	4.76	25	.02	20	
11A	.00967	0.941	5.09	0	.01-0.1	16	
11B	.0111	0.978	4.07	100,8	.01	13	
11C	.0115	0.954	6.40	-72	.01-0.1	17	
11D	.00984	0.986	4.11	100	.01-0.1	14	
11E	.00984	0.923	4.86	0	.01-0.1	18	
11F	.00816	0.937	3.55	100,8	.01	12	
12A	.0117	0.973	6.40	-72	.01-0.1	16	
12B	.0111	0.956	3.52	100	.01-0.1	17	

Specimen	Area of Cross Section in. <sup>2</sup>	Gauge length in.	LY P.S.I. x 10 <sup>4</sup>	Testing Temp. °C	Crosshead Speed in.min. <sup>-1</sup>	Approx. Uniform Deformation %	Remarks
12C	.0115	0.951	4.61	0	.01-0.1	14	
12D	.0115	0.965	3.19	100,8	.01	14	
12E	.0107	0.912	6.18	-72	.01-0.1	15	
12F	.00967	0.956	3.26	100	.01-0.1	15	
13A	.0100	0.928	4.80	0	.01-0.1	15	
13B	.0109	1.027	6.36	-72	.01-0.1	13	
13C	.0104	0.954	3.65	100	.01-0.1	15	
13D	.0115	0.940	4.54	0	.01-1.0	14	
13E	.0106	0.917	6.27	-72	.01-1.0	13	
13F	.00984	0.915	3.57	100	.01-0.1	13	

B. Single Crystals

Specimen	Area of Cross Section in. <sup>2</sup>	Gauge Length in.	Temperature °C	Crosshead Speed in.min. <sup>-1</sup>	Approx. Uniform Elongation %	Remarks
4A	.00709	.972	-	-	-	Damaged during mounting.
4B	.00785	0.991	100,8	.01	12	non axial loading
4C	.00818	0.936	25	.002-.02	10	
5A	.0106	0.937	25	.01-0.1	19	Twinning observed
5B	.0104	0.933	-72	.01-0.1	19	
5C	.00833	0.967	100,8	.01	15	
5D	.00968	0.950	100	.01-0.1	10	
6A	.00664	0.972	100	.01-0.1	26	
6B	.00566	0.910	100	.01-0.1	23	
6C	.00738	0.955	100,66	.01	12	
6D	.00849	0.917	100,-26	.01-0.1	14	
6E	.00832	0.931	-19	.01-0.1	14	
7A	.00753	0.953	0	.01-0.1	10	
7B	.00899	0.975	100,-72	.01	11	
7C	.00967	0.987	-195	.01-0.1	4	
7D	.0119	0.947	0,-72	.01	8	
7E	.0111	0.914	-72	.01-0.1	17	

APPENDIX III

A. Precision of Measurements

1. Grain Size Measurements

Taking the batch of specimens 13 A, B and C as a typical example, the precision of the measurements of the mean grain diameter can be estimated.

Define:

$d^0$  = calculated mean grain diameter

$d_i$  = diameter from the  $i^{th}$  measurement

$v_i$  = the residual ( $d_0 - d_i$ ).

Measurement	$d^0$ (microns)	$d_i$ (microns)	$ v_i $ (microns)
1	26.1	23.3	2.8
2	26.1	30.0	3.9
3	26.1	22.6	3.5
4	26.1	27.2	1.1
5	26.1	27.5	1.4
6	26.1	26.4	0.3

$$\sum_{i=1}^n |v_i| = 13.0$$

The probable error of the mean is calculated from Peter's formula:

$$\begin{aligned}
 P. E. &= \frac{.845}{\sqrt{n(n-1)}} \sum_{i=1}^n v_i && i = 1, 2, \dots, n \\
 &= \frac{.845}{\sqrt{6 \times 5}} \times 13.0 = 2.0
 \end{aligned}$$

Hence the mean grain diameter is

$$d_0 = 26.1 \pm 2.0 \text{ microns}$$

From these calculations it is apparent that the precision of the grain size measurements is about 8%.

## 2. Tensile Testing

The Instron Operating Instructions state that the accuracy of the load weighing system is better than 0.5% irregardless of the range in use. This is about the same as the accuracy in reading the chart which is about  $\pm 0.2$  of the smallest scale division.

### Sample calculation for the lower yield stress

Assume the following typical values:

$$F_{LY} = 400 \text{ lb. (load at the lower yield point)}$$

$$d = 0.1 \text{ in. (diameter of specimen)}$$

$$\sigma_{LY} = \frac{F_{LY}}{\frac{\pi d^2}{4}}$$

Differentiating logarithmically:

$$\frac{\delta \sigma_{LY}}{\sigma_{LY}} = \frac{\delta F_{LY}}{F_{LY}} + 2 \frac{\delta d}{d}$$

$$\text{Accuracy of } F_{LY} = \pm .2 \text{ lb.}$$

$$\text{Accuracy of } d = \pm .001''$$

The maximum error is:

$$\frac{\delta \sigma_{LY}}{\sigma_{LY}} = \frac{2}{400} + 2 \frac{.001}{.1} = .025 \text{ or } 2.5\%$$

The accuracy of the measurements of  $\Delta \tau_a$  is of principal concern. The smaller  $\Delta \tau_a$ , the more difficult a precise measurement will be.

This is evident in the plots in Figure (19) where the high temperature plots show the greatest scatter. The accuracy is estimated by:

$$\frac{\delta(\Delta\tau_a)}{\Delta\tau_a} = \frac{\delta(\tau_{a2}) + \delta(\tau_{a1})}{\Delta\tau_a}$$

At 100°C the specimens were generally tested at 500 lb. full scale deflection on the Instron.

$$\text{Hence } \delta\tau_{a2} = \delta\tau_{a1} = \pm 1 \text{ lb.}$$

$$\Delta\tau_a \approx 13 \text{ lb.}$$

$$\frac{\delta(\Delta\tau_a)}{\Delta\tau_a} = \frac{2}{13} \approx 15\%$$

This, of course, is a maximum estimate as the errors could compensate for each other.

Errors in the calculations of the rate parameters cannot be easily estimated without knowing the exact shape of the force - distance curve. The scatter in the plots of  $\Delta Q$  against temperature (Figure 24b) and in calculations of  $\Delta Q$  by different methods serves as a rough measure of the accuracy. From these comparisons one might expect our estimations of  $\Delta Q$  and  $H^{\circ}$  to be out as much as 25%. However, this is still adequate for determining a mechanism of flow since the theoretical calculations are probably not much more precise than this.

VIII. BIBLIOGRAPHY

1. Hall, E. O., Proc. Phys. Soc. Lond. B 64 747, (1951).
2. Petch, N. J., J. Iron and Steel Inst., 174 25, (1953).
3. Cracknell, A., Petch, N. J., Acta Met. 3 186, (1955).
4. Heslop, J., Petch, N. J., Phil. Mag. 1 866, (1956).
5. Conrad, H., Schoeck, G., Acta Met. 8 791, (1960).
6. Petch, N. J., Phil Mag. 3 1089, (1958).
7. Cottrell, A. H., Trans. A. I. M. E., 212 192, (1958).
8. Basinski, Z. S., Phil. Mag. 4 393, (1959).
9. Conrad, H., Wiedersich, H., Acta Met. 8 128, (1960).
10. Mordike, B. L., Haasen, P., Phil. Mag. 7 459, (1962).
11. Gregory, D. P., Stroh, A. N., Rowe, G. H., to be published.
12. Basinski, Z. S., Christian, J. W., Aust. J. Phys. 13 299, (1960).
13. Mordike, B. L., Z. Metallkunde 9 586, (1962).
14. Conrad, H., J. Iron and Steel Inst. 198 364, (1961).
15. Conrad, H., Phil. Mag. 5 745, (1960).
16. Conrad, H., To be published.
17. Snowball, R. F., M.A. Sc. Thesis, University of British Columbia, (1961).
18. Fraser, R. W., M. A. Sc. Thesis, University of British Columbia, (1960).
19. Conrad, H., Frederick, S., Acta Met. 10 1013, (1962).
20. Hirsch, P. B., Phil. Mag. 7 67, (1962).
21. Mott, N. F., Trans. A. I. M. E. 218 962, (1960).
22. Kuhlmann-Wilsdorf, D., Trans. A. I. M. E., 224 1047, (1962).
23. Cottrell, A. H., Dislocations and Plastic Flow in Crystals, Oxford University Press, (1953), page 134.
24. Low, J. R., Guard, R. W., Acta Met., 7 171, (1959).

BIBLIOGRAPHY Continued

25. Johnston, W. G., Gilman, J. J., J. Appl. Phys. 31 632 (1960).
26. Low, J. R., Turkalow, A. M. Acta Met., 10 362, (1962).
27. Stein, D. F., Low, J. R., J. Appl. Phys. 31 362, (1960).
28. Read, W. T., Dislocations in Crystals, McGraw Hill, N. Y., (1963), Page 46.
29. Seeger, A., Phil. Mag. 46, 1194, (1955).
30. Martinson, R. H., M. A. Sc. Thesis, University of British Columbia, (1963).
31. Makin, M. J., Phil. Mag. 3 287, (1958).
32. Birnbaum, H. K., Acta Met. 9 320, (1961).
33. Schoeck, G., Seeger, A., Acta Met. 7 469, (1959).
34. Frank, F. C., Il Nuovo Cimento 7 Supp. 1-2, 386, (1958).